

Last interglacial ocean changes in the Bahamas: climate teleconnections between low and high latitudes

Anastasia Zhuravleva¹ and Henning A. Bauch²

¹Academy of Sciences, Humanities and Literature, Mainz, c/o GEOMAR Helmholtz Centre for Ocean Research, Wischhofstrasse 1-3, Kiel, 24148, Germany

²Alfred Wegener Institute, Helmholtz Centre for Polar and Marine Research c/o GEOMAR Helmholtz Centre for Ocean Research, Wischhofstrasse 1-3, Kiel, 24148, Germany

Correspondence to: Anastasia Zhuravleva (azhuravleva@geomar.de)

Abstract. Paleorecords and modeling studies suggest that instabilities in the Atlantic Meridional Overturning Circulation (AMOC) strongly affect the low-latitude climate, namely via feedbacks on the Atlantic Intertropical Convergence Zone (ITCZ). Despite pronounced millennial-scale climatic variability documented in the subpolar North Atlantic during the last interglacial (MIS 5e), studies on the cross-latitudinal teleconnections remain to be very limited, precluding full understanding of the mechanisms controlling subtropical climate evolution across the last warm cycle. Here, we present new planktic foraminiferal assemblage data combined with $\delta^{18}\text{O}$ values in surface and thermocline-dwelling foraminifera from the Bahama region, which is ideally suited to study past changes in subtropical ocean and atmosphere. Our data reveal that the peak sea surface warmth during early MIS 5e was intersected by an abrupt millennial-scale cooling/salinification event, which was possibly associated with a sudden southward displacement of the mean annual ITCZ position. This atmospheric shift, which could have left its imprint on the low-latitude upper ocean properties, is ascribed to the transitional climatic regime of early MIS 5e characterized by persistent ocean freshening in the high latitudes and, therefore, an unstable AMOC mode.

Deleted: C

Deleted: The last interglacial (MIS 5e)

Deleted: and its impact on

Deleted: cycle at Little Bahama Bank:

Deleted: the

Deleted: A history of climate and sea-level changes

Deleted: Shallow-water sediments of the Bahama region containing the last interglacial (MIS 5e) are ideal to investigate the region's sensitivity to past climatic and sea level changes.

Deleted: new faunal

Deleted: shifts in the ITCZ

Deleted: , isotopic and XRF-sediment core data from the northern slope of the Little Bahama Bank. The results suggest that the bank top remained flooded across the last interglacial "plateau", ~129-117 ka, arguing for a relative sea level above -6 m for this time period. In addition, climatic variability, which today is closely coupled with movements of the intertropical convergence zone (ITCZ), is interpreted based on stable isotopes and foraminiferal assemblage records. During early MIS 5e, the mean annual ITCZ position moved northward in line with increased solar forcing and a recovered Atlantic Meridional Overturning Circulation (AMOC). The early MIS 5e warmth peak was intersected, however, by a millennial-scale cooling event.

Deleted: tropical

Deleted: ,

Deleted: high-latitude

Deleted: thereby

Deleted: ,

Deleted:

Deleted: Our shallow-water records from the Bahamas persuasively demonstrate that not only was there a tight relation between last interglacial sea level history and ice volume changes, via the atmospheric forcing we could further infer an intra-interglacial connectivity between the polar and subtropical latitudes that left its imprint also on the ocean circulation.

1 Introduction

In the low-latitude North Atlantic, wind patterns, precipitation-evaporation balance as well as sea surface temperatures (SSTs) and salinities (SSSs) are strongly dependent on the position of the Atlantic Intertropical Convergence Zone (ITCZ) and its associated rainfall (Peterson and Haug, 2006). Based on paleorecords and modelling studies, past positions of the ITCZ are thought to be related to the interhemispheric thermal contrast changes of which could be driven by two principal mechanisms: the precessional cycle and, associated with it, a cross-latitudinal distribution of solar insolation and millennial-scale climatic variability brought about by Atlantic Meridional Overturning Circulation (AMOC) instabilities (Wang et al., 2004; Broccoli et al., 2006; Arbuszewski et al., 2013; Schneider et al., 2014). Specifically, millennial-scale cold events in the high northern latitudes were linked with reduced convection rates of the AMOC, accounting for both a decreased oceanic transport of the tropical heat towards the north and a southward shift of the mean annual position of the ITCZ (Vellinga and Wood, 2002; Chiang et al., 2003; Broccoli et al., 2006). Reconstructions from the low-latitude North Atlantic confirm southward displacements of the ITCZ coeval with AMOC reductions and reveal a complex hydrographic response within the upper water column, generally suggesting an accumulation of heat and salt in the (sub)tropics (Schmidt et al., 2006a; Carlson et al., 2008; Bahr et al., 2011; 2013). There are, however, opposing views on the subtropical sea surface development at times of high-latitude cooling events. While some studies suggest stable or increasing SSTs (Schmidt et al., 2006a; Bahr et al., 2011; 2013), others imply an atmospheric-induced (evaporative) cooling (Chang et al., 2008; Chiang et al., 2008).

The last interglacial (MIS 5e), lasting from about ~130 to 115 thousand years before present (hereafter [ka]), is often referred to as a warmer-than-preindustrial interval, associated with significantly reduced ice sheets and a sea level rise up to 6-9 meters above the present levels (Dutton et al., 2015; Hoffman et al., 2017). This time period has attracted a lot of attention as a possible analog for future climatic development as well as a critical target for validation of climatic models (Masson-Delmotte et al., 2013). Proxy data from the North Atlantic demonstrate that the climate of the last interglacial was relatively unstable, involving one or several cooling events (Maslin et al., 1998; Fronval and Jansen, 1997; Bauch et al., 2012; Irvali et al., 2012, 2016; Zhuravleva et al., 2017a, b). This climatic variability is thought to be strongly related to changes in the AMOC strength (Adkins et al., 1997). Thus, recent studies reveal that the AMOC abruptly recovered after MIS 6 deglaciation (Termination 2 or T2), i.e., at the onset of MIS 5e, at ~129 ka, but it was interrupted around 127-126 ka (Galaasen et al., 2014; Deaney et al., 2017). Despite the pronounced millennial-scale climatic variability documented in the high northern latitudes, studies on the cross-latitudinal links are very limited (but see e.g., Cortijo et al., 1999; Schwab et al.,

Deleted: ¶

Deleted: is

Deleted: strongly

Deleted: are associated

Deleted: ,

Deleted: are consistent with

Deleted: s

Deleted: coolings

Deleted: :

Deleted: w

Deleted: during MIS6 deglaciation (Termination 2)

2013; Kandiano et al., 2014; Govin et al., 2015; Jiménez-Amat and Zahn, 2015). This precludes the full understanding of the mechanisms, regulating subtropical climate across the last interglacial, i.e., insolation, oceanic and/or atmospheric forcing versus high-low-latitudes feedbacks.

Given its critical location near the origin of the Gulf Stream, sediments from downslope the shallow-water carbonate platforms of the Bahamian archipelago (Fig. 1) have been previously investigated in terms of oceanic and atmospheric variability (Slowey and Curry, 1995; Roth and Reijmer, 2004, 2005; Chabaud et al., 2016). However, a thorough study of the last interglacial climatic evolution underpinned by a critical stratigraphical insight is lacking so far. Here, a sediment record from the Little Bahama Bank (LBB) region is investigated for possible links between the AMOC variability and the ITCZ during the last interglacial cycle. Today the LBB region lies at the northern edge of the influence of the Atlantic Warm Pool, which expansion is strongly related to the ITCZ movements (Wang and Lee, 2007; Levitus et al., 2013), making our site particularly sensitive to monitor past shifts of the ITCZ. Given that geochemical properties of marine sediments around carbonate platforms vary in response to sea level fluctuations (e.g., Lantzsich et al., 2007), X-ray fluorescence (XRF) data are being used together with stable isotope and faunal records to strengthen the temporal framework. Planktic foraminiferal assemblage data complemented by $\delta^{18}\text{O}$ values, measured on surface- and thermocline-dwelling foraminifera, are employed to reconstruct the upper ocean properties (stratification, trends in temperature and salinity), specifically looking at mechanisms controlling the foraminiferal assemblages. Assuming a coupling between foraminiferal assemblage data and past mean annual positions of the ITCZ (Poore et al., 2003; Vautravers et al., 2007), our faunal records are then looked at in terms of potential geographical shifts of the ITCZ. Finally, we compare our new proxy records with published evidence from the regions of deep water formation to draw further conclusions on the subpolar forcing on the low-latitude climate during MIS 5e.

2 Regional Setting

2.1 Hydrographic context

Core MD99-2202 (27°34.5' N, 78°57.9' W, 460 m water depth) was taken from the upper northern slope of the LBB, which is the northernmost shallow-water carbonate platform of the Bahamian archipelago. The study area is at the western boundary of the wind-driven subtropical gyre (STG), in the vicinity to the Gulf Stream (Fig. 1a). The Gulf Stream supplies both heat and salt to the high northern latitudes thereby constituting the upper cell of the AMOC.

Deleted: This globally warmer-than-preindustrial interval is associated with significantly reduced ice sheets and a sea level rise up to 6-9 meters above the present levels (Dutton et al., 2015; Hoffman et al., 2017). However, controversy still exists

Deleted: regarding the initiation and duration of the sea level highstand as well as about any sea level variability within that time period (Hearty et al., 2007; Kopp et al., 2009; Grant et al., 2012; Masson-Delmotte et al., 2013). Also, the spatial coverage of the existing sea surface temperature (SST) reconstructions is insufficient to allow for a robust understanding of the climatic forcing at play during the last interglacial. ... [1]

Deleted: records

Deleted: from

Deleted: e Bahama Bank region

Deleted: climatic

Deleted: , ocean circulation

Deleted: , sea level change and sediment diagenesis

Deleted: Henderson et al., 2000;

Deleted: Slowey et al., 2002;

Deleted: Chabaud, 2016

Deleted: ... [2]

Deleted: e

Deleted: deduced from periplatform oozes

Deleted: t

Deleted: were

Deleted: were

Deleted: Considering

Deleted: the inferred

Deleted: the

Deleted: in the past

Deleted: were

Deleted: interpreted

Deleted: ,

Deleted: , as previous authors mainly worked on timescale [3]

Deleted:

Deleted:

Deleted: from

Deleted: e

Deleted: the northern slope of the LBB

Deleted: western boundary current of the N. Atlantic STG [4]

Deleted: 1A

Deleted: and

Deleted: Atlantic Meridional Overturning Circulation (

Deleted:)

Deleted: It originates from the Florida Current after it... [5]

225 In the western subtropical North Atlantic two distinctly different layers can be distinguished within the upper 500
 226 m of the water column (Fig. 1c). The uppermost mixed layer (upper 50-100 m) is occupied by warm and
 227 comparatively fresh waters ($T > 24^{\circ}\text{C}$, $S < 36.4$ psu), predominantly coming from the equatorial Atlantic (Schmitz
 228 and McCartney, 1993; Johns et al., 2002). Properties of this water mass vary significantly on seasonal timescales
 229 and are closely related to the latitudinal migration of the ITCZ (Fig. 1b). During boreal winter (December-April),
 230 when the ITCZ is in its southernmost position, the Bahama region is dominated by relatively cool, stormy weather
 231 with prevailing northern and northeastern trade winds and is affected by cold western fronts, that increase
 232 evaporation and vertical convective mixing (e.g., Wilson and Roberts, 1995). During May to November, as the
 233 ITCZ moves northward, the LBB region is influenced by relatively weakened trade winds from the east and
 234 southeast, increased precipitation and very warm waters of the Atlantic Warm Pool ($T > 28.5^{\circ}\text{C}$), which expand
 235 into the Bahama region from the Caribbean Sea and the equatorial Atlantic (Stramma and Schott, 1999; Wang
 236 and Lee, 2007; Levitus et al., 2013).

237 The mixed layer is underlain by the permanent thermocline, which is comprised of a homogeneous pool of
 238 comparatively cool and salty ($T < 24^{\circ}\text{C}$, $S > 36.4$ psu) water (Schmitz and Richardson, 1991). These “mode”
 239 waters are formed in the North Atlantic STG through wintertime subduction of surface waters generated by wind-
 240 driven Ekman downwelling and buoyancy flux (Slowey and Curry, 1995).

242 2.2 Sedimentological context

243 Along the slopes of the LBB, sediments are composed of varying amounts of sedimentary input from the platform
 244 top and from the open ocean, depending on the global sea level state (Droxler and Schlager, 1985; Schlager et al.,
 245 1994). During interglacial highstands, when the platform top is submerged, the major source of sediment input is
 246 the downslope transport of fine-grained aragonite needles, precipitated on the platform top. This material
 247 incorporates significantly higher abundances of strontium (Sr), than found in pelagic-derived aragonite (e.g.,
 248 pteropods) and calcite material from planktic foraminifera and coccoliths (Morse and MacKenzie, 1990). Given
 249 that in the periplatform interglacial environment modifications of the aragonite content due to sea floor dissolution
 250 and/or winnowing of fine-grained material are minimal (Droxler and Schlager, 1985; Schlager et al., 1994; Slowey
 251 et al., 2002), thicker sediment packages accumulate on the slopes of the platform, yielding interglacial climate
 252 records of high resolution (Roth and Reijmer, 2004; 2005). During glacial lowstands on the contrary, as the LBB
 253 bank top is exposed, aragonite production is limited, sedimentation rates are strongly reduced and coarser-grained

Deleted: .

Deleted: intertropical convergence zone (ITCZ)

Deleted:) (Fig. 1B-C)

Deleted: a

Deleted: pool of waters ($T > 28^{\circ}\text{C}$) which expands into the Bahama region from the Caribbean Sea and the equatorial Atlantic (Stramma and Schott, 1999; Wang and Lee, 2007; Levitus et al., 2013). Today, the LBB region lies at the northern edge of the influence of tropical pool waters, making our site particularly sensitive to monitor past shifts of the ITCZ.

Deleted: a

Deleted: layer

Deleted: $12 <$

Deleted: .

Deleted: driven

Deleted: from

Deleted: s

Deleted: Typical

Deleted: As in a

Deleted: for

Deleted: as well as by

Deleted: ; Chabaud et al., 2016

Deleted: whereas

Deleted: are

Deleted: d

Deleted: producing

Deleted: high resolution

Deleted: interglacial climate

283 consolidated sediments are formed from the pelagic organisms (Droxler and Schlager, 1985; Slowey et al., 2002;
284 Lantzsich et al., 2007).

285

286 3 Methods

287 3.1 Foraminiferal counts and stable isotopes analyses

288 Planktic foraminiferal assemblages were counted on representative splits of the 150-250 µm fraction containing
289 at least 300 individual specimens. Counts were also performed in the >250 µm fraction. The census data from the
290 two size fractions were added up and recalculated into relative abundance of planktic foraminifera in the fraction
291 >150 µm. Faunal data were obtained at each 2 cm for the core section between 508.5 and 244.5 cm and at each
292 10 cm between 240.5 and 150.5 cm. According to a standard practice, *Globorotalia menardii* and *Globorotalia*
293 *tumida* as well as *Globigerinoides sacculifer* and *Globigerinoides trilobus* were grouped together, and referred to
294 as *G. menardii* and *G. sacculifer*, respectively (Poore et al., 2003; Kandiano et al., 2012; Jentzen et al., 2018).

295 New oxygen isotope data were produced at 2 cm steps using ~10-30 tests of *Globorotalia truncatulinoides* (dex)
296 and ~5-20 tests of *Globorotalia inflata* for depths 508.5-244.5 cm and 508.5-420.5 cm, respectively. Analyses
297 were performed using a Finnigan MAT 253 mass spectrometer at the GEOMAR Stable Isotope Laboratory.
298 Calibration to the Vienna Pee Dee Belemnite (VPDB) isotope scale was made via the NBS-19 and an internal
299 laboratory standard. The analytical precision of in-house standards was better than 0.07‰ (1σ) for δ¹⁸O. Isotopic
300 data derived from the deep-dwelling foraminifera *G. truncatulinoides* (dex) and *G. inflata* could be largely
301 associated with the permanent thermocline and linked to winter conditions (Groeneveld and Chiessi, 2011;
302 Jonkers and Kučera, 2017; Jentzen et al., 2018). However, as calcification of their tests starts already in the mixed
303 layer and continues in the main thermocline (Fig. 1c), the abovementioned species are thought to accumulate in
304 their tests hydrographic signals from different water depths (Groeneveld and Chiessi, 2011; Mulitza et al., 1997).

305

306 3.2 XRF scanning

307 XRF analysis was performed in two different runs using the Aavatech XRF Core Scanner at Christian-Albrecht
308 University of Kiel (for technical details see Richter et al., 2006). To obtain intensities of elements with lower
309 atomic weight (e.g., calcium (Ca), chlorine (Cl)), XRF scanning measurements were carried out with the X-ray
310 tube voltage of 10 kv, the tube current of 750 µA and the counting time of 10 seconds. To analyze heavy elements
311 (e.g., iron (Fe), Sr), the X-ray generator setting of 30 kv and 2000 µA and the counting time of 20 seconds were
312 used; a palladium thick filter was placed in the X-ray tube to reduce the high background radiation generated by

Deleted: ¶

Deleted: i

Deleted: (Poore et al., 2003; Kandiano et al., 2012; Chabaud, 2016)

Deleted: Deep-dwelling foraminifera *G. truncatulinoides* and *G. inflata* are found in greatest abundances at the base of the seasonal thermocline (100-200 m), under environmental stress, e.g., temperatures warmer than 16°C, however, the species can migrate to greater depths (Cléroux et al., 2007). A

Deleted: ing

Deleted: Also, isotopic data derived from *G. truncatulinoides* and *G. inflata* bear a cold-season weighted signal, as these species are abundant in the N. Atlantic STG during winter-spring time (Jonkers and Kučera, 2015). ¶

Deleted: X-ray fluorescence (

Deleted:)

Deleted:

the higher source energies. XRF Core Scanner data were collected directly from the split core sediment surface, that had been flattened and covered with a 4 µm-thick ULTRALENE SPEXCerti Prep film to prevent contamination of the measurement unit and desiccation of the sediment (Richter et al., 2006; Tjallingii et al., 2007). The core section between 150 and 465 cm was scanned at 3 mm step size, whereas the coarser-grained interval between 465 and 600 cm was analyzed at 10 mm resolution.

To account for potential biases related to physical properties of the sediment core (see e.g., Chabaud, 2016), XRF intensities of Sr were normalized to Ca, the raw total counts of Fe and Sr were normalized to the total counts of the 30kv-run; counts of Ca and Cl were normalized to the total counts of 10kv-run, excluding Rh intensity, because this element intensities are biased by the signal generation (Bahr et al., 2014).

4 Age model

By using our foraminiferal assemblage data, we were able to refine the previously published age model of core MD99-2202 (Lantzsich et al., 2007). To correctly frame MIS 5e, stratigraphic subdivision of the unconsolidated aragonite (Sr)-rich sediment package between 190 and 464 m is essential (Fig. 2). In agreement with Lantzsich et al. (2007), we interpret this core section to comprise MIS 5, which is supported by key biostratigraphic markers used to identify the well-established faunal zones of late Quaternary (Ericson and Wollin, 1968). Thus, the last occurrence of *G. menardii* at the end of the aragonite-rich sediment package is in agreement with the estimated late MIS 5 age (ca. 80-90 ka; Boli and Saunders, 1985; Slowey et al., 2002; Bahr et al., 2011; Chabaud, 2016). The coherent variability in the ~200-300 cm core interval, observed between aragonite content and relative abundances of warm surface-dwelling foraminifera of *Globigerinoides* genus (*G. ruber*, white and pink varieties, *G. conglobatus* and *G. sacculifer*), points to simultaneous climate and sea level-related changes and likely reflects the warm/cold substages of MIS 5. The identified substages were then correlated with the global isotope benthic stack LS16 (Lisiecki and Stern, 2016) using AnalySeries 2.0.8 (Paillard et al., 1996). Further, boundaries between MIS 6/5e and 5e/5d as well as the penultimate glaciation (MIS 6) peak, defined from $\delta^{18}\text{O}$ record of *G. ruber* (white), were aligned to the global benthic stack (Lisiecki and Stern, 2016).

Given that sedimentation rates at the glacial/interglacial transition could have changed drastically due to increased production of Sr-rich aragonite material above the initially flooded carbonate platform top (Roth and Reijmer, 2004), we applied an additional age marker to better frame the onset of the MIS 5e "plateau" (Masson-Delmotte et al., 2013) and to allow for a better core-to-core comparison. Thus, we tied the increased relative abundances of warm surface-dwelling foraminifera of *Globigerinoides* genus, which coincides with the rapid decrease in

Deleted: E SPEXCerti Prep

Deleted: (Fig. 2)

Deleted: All data will be made available in the online database PANGAEA (www.pangaea.de). ¶

Deleted: aragonite

Deleted: 3

Deleted: at

Deleted: s

Deleted: and *G. menardii* flexuosa

Deleted: are

Deleted:

Deleted: between ~200-300 cm

Deleted: detected

Deleted: ; Chabaud et al., 2016

foraminiferal $\delta^{18}\text{O}$ record at 456 cm, with the onset of MIS 5e “plateau” at ~129 ka (Masson-Delmotte et al., 2013). This age is in good agreement with many marine and speleothem records, dating a rapid post-stadial warming and monsoon intensification to 129-128.7 ka (Govin et al., 2015; Jiménez-Amat and Zahn, 2015; Deaney et al., 2017), coincident with the sharp methane increase in the EPICA Dome C ice core (Loulergue et al., 2008; Govin et al., 2012). Although we do not apply a specific age marker to frame the decline of the MIS 5e “plateau”, the resulting decrease in the percentage of warm surface-dwelling foraminifera of *Globigerinoides* genus as well as the initial increase in the planktic $\delta^{18}\text{O}$ values dates back to ~117 ka (Figs. 3-5), which broadly coincides with the cooling over Greenland (NGRIP community members, 2004). A similar subtropical-polar climatic coupling was proposed in earlier studies from the western North Atlantic STG (e.g., Vautravers et al., 2004; Schmidt et al., 2006a; Bahr et al., 2013; Deaney et al., 2017).

5 Results

5.1 XRF data in the lithological context

In Fig. 3, XRF-derived elemental data are plotted against lithological and sedimentological records. Beyond the intervals with low Ca counts and correspondingly high Cl intensities (at 300-325 cm and 395-440 cm), Ca intensities do not vary significantly, which is in line with a stable carbonate content of about 94 % Wt (Lantzsche et al., 2007). Our Sr record closely follows the aragonite curve, demonstrating that the interglacial mineralogy is dominated by aragonite. Beyond the intervals containing reduced Ca intensities, a good coherence between Sr/Ca and aragonite content is observed. The rapid increase in Sr/Ca and aragonite is found at the end of the penultimate deglaciation (T2), coeval with the elevated absolute abundances of *G. menardii* per sample (Fig. 3). The gradual step-like Sr/Ca and aragonite decrease characterizes both the glacial inception and the later MIS 5 phase. Intensities of Fe abruptly decrease at the beginning of the last interglacial, but gradually increase during the glacial inception (Fig. 4). Between ~112 and 114.5 ka, the actual XRF measurements were affected by a low sediment level in the core tube.

5.2 Climate-related proxies

To calculate $\delta^{18}\text{O}$ gradients across the upper water column, we also used the published $\delta^{18}\text{O}$ data by Lantzsche et al. (2007), which were measured on the surface-dwelling foraminifera *G. ruber* (white). These isotopic data can be generally associated with mean annual conditions (Tedesco et al., 2007), however, during colder time intervals productivity peak of *G. ruber* (white) could shift towards warmer months, leading to underestimation of the actual

Deleted: Galaasen et al., 2014;

Deleted: 4

Deleted: .

Deleted: 2

Deleted: physical

Deleted: properties

Deleted: to

Deleted: and the grain size data

Deleted: Termination 2,

Deleted: 4

Deleted: 5D

Deleted: At ~120 ka (355 cm), a minor but clear increase in Sr intensities goes along with the change in aragonite and grain-size (Figs. 2 and 4), arguing that this feature is not a signal artefact but represents a significant sedimentological shift.

Deleted: in

Deleted: $\delta^{18}\text{O}$ values

Deleted: could

environmental change (Schmidt et al., 2006a, b; Jonkers and Kučera, 2015). During the penultimate glacial maximum (MIS 6), $\delta^{18}\text{O}$ gradients between *G. ruber* (white) and *G. truncatulinoides* (dex) and *G. inflata* are very low (Fig. 4), succeeded by a gradually increasing difference across T2, ~135-129 ka. Changes in the isotopic gradient between surface- and thermocline-dwelling foraminifera closely follow variations in the relative abundances of *G. truncatulinoides* (dex) and *G. inflata* (Fig. 4). Across MIS 5e species of *Globigerinoides* genus dominate the total assemblage, however, significant changes in the proportions of three main *Globigerinoides* species are observed (Fig. 5): *G. sacculifer* and *G. ruber* (pink) essentially dominate the assemblage during early MIS 5e (129-124 ka), whereas *G. ruber* (white) proportions are at their maximum during late MIS 5e (124-117 ka). At around 127 ka, all $\delta^{18}\text{O}$ records abruptly increase together with a reappearance of *G. inflata* (Fig. 4) and a relative abundance decrease of *G. ruber* (pink) and *G. sacculifer* (Fig. 5). After 120 ka, $\delta^{18}\text{O}$ values in *G. ruber* (white) and *G. truncatulinoides* (dex) become unstable (Fig. 4). That instability coincides with an abrupt drop in *G. sacculifer* relative abundances (Fig. 5).

6 Discussion

6.1 Platform sedimentology and relative sea level change

The modern LBB lagoon is shallow with an average water depth between 6-10 m (Williams, 1985). Despite some possible isostatic subsidence of 1-2 m per hundred thousand years (Carew and Mylroie, 1995), the LBB region is generally regarded as tectonically stable (Hearty and Neumann, 2001). Considering this, a relative sea level (RSL) rise above -6 m of its present position is required to completely flood the platform top and allow for a drastic increase in platform-derived (Sr-rich aragonite) sediment particles (Neumann and Land, 1975; Droxler and Schlager, 1985; Schlager et al., 1994; Carew and Mylroie, 1997). As such, the LBB flooding periods exceeding -6 m RSL can be defined from downcore variations in Sr/Ca intensity ratio (Chabaud et al., 2016).

While our Sr record likely represents a non-affected signal because of good coherence with the aragonite record, some of the Ca intensity values are reduced due to increased seawater content, as evidenced by simultaneously measured elevated Cl intensities (Fig. 3). Because enhanced seawater content in the sediment appears to reduce only Ca intensities, which leaves elements of higher atomic order (e.g., Fe, Sr) less affected (Tjallingii et al., 2007; Hennekam and de Lange, 2012), normalization of Sr counts to Ca results in very high Sr/Ca intensity ratios across the Cl-rich intervals. Regardless of these problematic intervals described above, the XRF-derived Sr/Ca values agree well with the actually measured aragonite values that it seems permissible to interpret them in terms of RSL variability.

Deleted: isotopic

Deleted: ,

Deleted: the major deglacial transition

Deleted: ,

Deleted: low isotopic gradients between *G. ruber* (white), *G. truncatulinoides* (dex) and *G. inflata* are consistent with high

Deleted: 5

Deleted: At the onset of MIS 5e, *G. ruber* (pink) and *G. sacculifer* relative abundances rise in a successive manner, with a rapid increase in *G. sacculifer* occurring c. 2 ka later than the rise in *G. ruber* (pink) proportions.

Deleted: ,

Deleted: *G. falconensis* and

Deleted: reappear

Deleted: , while

Deleted: s

Deleted: become reduced

Deleted: s

Deleted: 5-6

Deleted: 5A-B

Deleted: is

Deleted: 6B

Deleted: M

Deleted: (

Deleted: ,

Deleted: vs. pelagic (Sr-poor calcite or aragonite)

Deleted: In shallow-water records from the Bahamas

Deleted: ,

Deleted: can be applied

Deleted: as a good proxy for relative sea level (RSL) change

Deleted: However, given that the measured intensities of Ca

Deleted: curve

Deleted: 2

Deleted: leaving measures of

Deleted: with

Deleted: numbers

Deleted: The general consistency of the measured Sr ... [7]

Deleted: Beyond

Deleted: curve

Deleted: and, thus,

Deleted: can

Deleted: be

Deleted: ed

Deleted: (Fig. 4)

525 Around 129 ka, Sr/Ca rapidly reach maximum values, indicating the onset of the LBB flooding interval with the
 526 inferred RSL above -6 m (Fig. 3). Absolute abundance of *G. menardii* per sample support the inferred onset of
 527 the flooding interval, since amounts of planktic foraminifera in the sample can be used to assess the relative
 528 accumulation of platform-derived versus pelagic sediment particles (Slowey et al., 2002). After *G. menardii*
 529 repopulated the (sub)tropical waters at the end of the penultimate glaciation (Bahr et al., 2011; Chabaud, 2016),
 530 its increased absolute abundances are found around Bahamas between ~131-129 ka. This feature could be
 531 attributed to a reduced input of fine-grained aragonite at times of partly flooded platform. Consequently, as the
 532 platform top became completely submerged, established aragonite shedding gained over pelagic input, thereby
 533 reducing the number of *G. menardii* per given sample. Our proxy records further suggest that the aragonite
 534 production on top of the platform was abundant until late MIS 5e (unequivocally delimited by foraminiferal $\delta^{18}\text{O}$
 535 and faunal data). The drop in RSL below -6 m only during the terminal phase of MIS 5e (~117-115 ka on our
 536 timescale) is corroborated by a coincident changeover in the aragonite content and an increase in absolute
 537 abundance of *G. menardii*, further supporting the hypothesis that aragonite shedding was suppressed at that time,
 538 causing relative enrichment in foraminiferal abundances.

539 The exact timing of the last interglacial global sea level peak is a rather controversial matter of debate as studies
 540 place it into either early (Grant et al., 2012; Lisiecki and Stern, 2016), mid or late MIS 5e (Hearty and Neumann,
 541 2001; Hearty et al., 2007; Kopp et al., 2009; O'Leary et al., 2013; Spratt and Lisiecki, 2016). Although the Bahama
 542 region is located quite away from the former Laurentide Ice Sheet, there still could have been some influence by
 543 glacio-isostatic adjustments, causing our RSL signals to deviate from the global sea level during MIS 5e (Stirling
 544 et al., 1998). Therefore, we refrain from making any further evaluation of this issue at this point.

546 6.2 Deglacial changes in the vertical water mass structure

547 Particularly high proportions of thermocline-dwelling foraminifera *G. inflata* and *G. truncatulinoides* (dex) are
 548 found off LBB during late MIS 6 and T2 (Fig. 4). To define mechanisms controlling the faunal assemblage, we
 549 look at $\delta^{18}\text{O}$ values in those foraminiferal species which document hydrographic changes across the upper water
 550 column, i.e., spanning from the uppermost mixed layer down to the permanent thermocline. The strongly reduced
 551 $\delta^{18}\text{O}$ gradients between surface-dwelling species *G. ruber* (white) and two thermocline-dwelling foraminifera *G.*
 552 *truncatulinoides* (dex) and *G. inflata* during T2 and particularly during late MIS 6 could be interpreted in terms
 553 of decreased water column stratification, a condition which is favored by thermocline-dwelling foraminifera (e.g.,
 554 Mulitza et al., 1997). Specifically, for *G. truncatulinoides* (dex), this hypothesis is supported by its increased

Deleted: as well as aragonite content

Deleted: s

Deleted: (Fig. 4D)

Deleted: .

Deleted: That

Deleted:

Deleted: 117

Deleted: the

Deleted: (per sample)

Deleted: Because

Deleted: not

Deleted: far

Deleted: and, thus,

Deleted: likely have

Deleted: d

Deleted: processes

Deleted: .

Deleted: ,

Deleted: could

Deleted: significantly

Deleted: actual eustatic

Deleted: change

Deleted: As such, Our data do not allow to make assumptions about the exact timing of the last interglacial sea level peak, which is controversially placed by different studies into either early (Grant et al., 2012; Lisiecki and Stern, 2016), mid or late MIS 5e (Hearty and Neumann, ... [8]

Deleted: ... [9]

Deleted: a

Deleted: ly placed by different studies into either early. [10]

Deleted: Termination 2

Deleted: various

Deleted: ,

Deleted: ing

Deleted: permanent

Deleted: In the first place

Deleted: ,

Deleted: The

Deleted: t

Deleted: different

Deleted: Isotopic gradients between $\delta^{18}\text{O}$ values in surfa [11]

Deleted: foraminifera during T2 are strongly reduced. [12]

Deleted: , in turn,

Deleted: for enhanced abundances of

Deleted: ,

abundance within the regions characterized by deep winter vertical mixing (Siccha and Kučera, 2017). Such environmental preference may be explained by species ontogeny, given that *G. truncatulinoides* (dex) requires reduced upper water column stratification to be able to complete its reproduction cycle with habitats ranging from c. 400-600 m to near-surface depths; in well-stratified waters, however, reproduction of *G. truncatulinoides* (dex) would be inhibited by a strong thermocline (Lohmann and Schweizer, 1990; Hilbrecht, 1996; Mulitza et al., 1997; Schmuker and Schiebel, 2000).

To explain the inferred reduced upper water mass stratification during late MIS 6 and T2, sea surface cooling/salinification and/or subsurface warming could be invoked (e.g., Zhang, 2007; Chiang et al., 2008). While Mg/Ca-based temperature estimations during late MIS 6, so far reveal cold subsurface conditions for the subtropical western North Atlantic (Bahr et al., 2011; 2013), it should be noted that species-specific signals (i.e., $\delta^{18}\text{O}$ values, Mg/Ca-ratios) could be complicated due to adaptation strategies of foraminifera, such as seasonal shifts in the peak foraminiferal tests flux and/or habitat changes (Schmidt et al., 2006a, b; Cléroux et al., 2007; Bahr et al., 2013; Jonkers and Kučera, 2015). However, further insights into the past hydrographic changes could be provided from the conspicuous millennial-scale reversion found at 131 ka (Fig. 4), associated with a shift towards lower surface-thermocline isotopic gradients (i.e., reduced stratification). When compared to the abrupt increase in *G. ruber* (white) $\delta^{18}\text{O}$ values at 131 ka, which indicates sea surface cooling or salinification, the isotopic response in thermocline-dwelling species remains rather muted. The latter could be explained either by foraminiferal adaptation strategies, stable subsurface conditions and/or incorporation of opposing signals during foraminiferal ontogenetic cycle that would mitigate the actual environmental change. Regardless of the exact mechanism, there is a good coherence between $\delta^{18}\text{O}$ values in *G. ruber* (white) and relative abundances of *G. inflata* and *G. truncatulinoides* (dex), suggesting a possible link between thermocline species abundance and conditions occurring nearer to the sea surface (Mulitza et al., 1997; Jonkers and Kučera, 2017). Specifically, steadily increasing upper water column stratification across glacial-interglacial transition could have suppressed reproduction of *G. truncatulinoides* (dex) and *G. inflata*, while the short-term stratification reduction at 131 ka may have promoted favorable conditions for the thermocline-dwelling species through sea surface cooling and/or salinification.

It should be noted, however, that stratification is not a sole mechanism for explaining variability in the thermocline-associated assemblage. Thus, while relative abundances of *G. inflata* become strongly reduced at the onset of MIS 5e, there is no such response in the *G. truncatulinoides* (dex) proportions (Fig. 4). Whereas *G. inflata* is generally regarded as subpolar to transitional species, preferring little seasonal variations in salinity (Hilbrecht,

Deleted: High abundances... of *G. truncatulinoides* (Fig. 5E) further support the hypothesis involving... within the regions characterized by reduced stratification and ... [13]

Deleted: is... may be explained by the ... [14]

Deleted: ,

Deleted: ,

Deleted: G

Deleted: g

Deleted: this species ... requires reduced upper water column stratification during winter time ... [15]

Deleted: changing ... habitats, ... [16]

Deleted: (Lohmann and Schweizer, 1990; Hilbrecht, 1996; Mulitza et al., 1997) ... [17]

Deleted: while

Deleted: I

Deleted: i

Deleted: however... however, . For instance, in the modern tropical Caribbean, ... reproduction of *G. truncatulinoides* (dex) would be... inhibited by a strong thermocline in well-stratified waters ... [18]

Deleted: ... sea surface cooling/salinification and/or subsurface warming could be invoked (e.g., Zhang, 2007; Chiang et al., 2008). At C of suppressed overturning during T2 (Deaney et al., 2017), the inferred decreased stratification could have resulted from sea surface cooling/salinification and/or subsurface warming (e.g., Zhang, 2007)... hile d... Mg/Ca-based direct... surface/subsurface ... emperature estimations across ... uring T2 and early MIS 5... ate MIS 6e... so far reveal warm/... old subsurface conditions for the subtropical western North... Atlantic (Bahr et al., 2011; 2013), it should be noted as ... hat species-specific temperature ... signals (i.e., $\delta^{18}\text{O}$ values, Mg/Ca-ratios) should be considered with caution, as they ... [19]

Deleted: ing... sea surface cooling or salinification, the isotopic response in thermocline-dwelling species is ... [20]

Deleted: for our subtropical settings ... possible link between thermocline species abundances... and conditions occurring nearer to the sea surface (Mulitza et al., 1997; Jonkers and Kučera, 2016 ... [21]

Deleted: Namely

Deleted:

Deleted: could

Deleted: for transitional to subpolar species *G. inflata*

Deleted: Alternatively, reduced water column stratification during winter could have led to a situation when calcification of the thermocline-dwelling foraminifera could have commenced in shallower and, therefore, relatively warmer waters, causing a lower isotopic gradient between shallow- and deep-dwelling foraminifera (Mulitza et al., 1997).

Deleted: noted

1996), *G. truncatulinoides* (dex) was shown to dwell in warmer temperatures (Siccha and Kučera, 2017) and occurs in small amounts also in the modern tropical Atlantic (Jentzen et al., 2018). However, an abrupt increase in the latter species proportions during the sea surface cooling/salinification event at ~127 ka (see further below), coupled with reduced upper water column stratification, supports the underlying “sea surface” control on the general abundance of *G. truncatulinoides* (dex). A southern position of the mean annual ITCZ during the penultimate (de)glaciation could be inferred based on previous studies (Yarincik et al., 2000; Wang et al., 2004; Schmidt et al., 2006a; Carlson et al., 2008; Arbuszewski et al., 2013; Bahr et al., 2013). By analogy with the modern atmospheric forcing in the region, a southern location of the ITCZ could have caused enhanced upper water column mixing and evaporative cooling through intensified trade winds (e.g., Wilson and Roberts, 1995). Acknowledging the fact that our study region lies too far north to be influenced by changes in the winter position of the ITCZ (Ziegler et al., 2008) – this would be of primary importance for modern-like winter-spring reproduction timing of *G. truncatulinoides* (dex) and *G. inflata* (Jonkers and Kučera, 2015) - we suggest that a southern location of the mean annual position of the ITCZ during the penultimate (de)glaciation could have facilitated favorable conditions for the latter species through generally strong sea surface cooling/salinification in the subtropical North Atlantic. Previous studies attributed increased Fe content in the Bahamas sediments to enhanced trade winds strength, given that siliclastic inputs by other processes than wind transport are very limited (Roth and Reijmer, 2004). Accordingly, elevated XRF-derived Fe counts in our record during T2 (Fig. 4) may support intensification of the trade winds and possibly increased transport of Saharan dust at times of enhanced aridity over Northern Africa (Muhs et al., 2007; Helmke et al., 2008). We, however, refrain from further interpretations of our XRF record due to a variety of additional effects that may have influenced our Fe-record (e.g., diagenesis, change in the source and/or properties of eolian inputs, sensitivity of the study region to atmospheric shifts, etc.).

6.3 MIS 5e climate in the subtropics: orbital versus subpolar forcing

Various environmental changes within the mixed layer (SST, SSS, nutrients) can account for the proportional change in different *Globigerinoides* species (Fig. 5). *G. sacculifer* – it makes up less than 10 % of the planktic foraminiferal assemblage around the LBB today (Siccha and Kučera, 2017) – is abundant in the Caribbean Sea and tropical Atlantic and commonly used as a tracer of tropical waters and geographical shifts of the ITCZ (Poore et al., 2003; Vautravers et al., 2007). Also, *G. ruber* (pink) shows rather coherent abundance maxima in the tropics, while no such affinity is observed for *G. ruber* (white) and *G. conglobatus* (Siccha and Kučera, 2017; Schiebel

Deleted: the overall

Deleted: in our subtropical settings

Deleted: inferred

Deleted: mean

Deleted:

Deleted: could be inferred based

Deleted: Previous studies from the western subtropical North Atlantic have shown that time periods with reduced AMOC strength are consistent with southward displacements of the ITCZ and its associated rainfall belt, causing sea surface salinification

Deleted:

Deleted: in the region through

Deleted: and

Deleted:

Deleted: produce

Deleted: As a southern mean position of the ITCZ is inferred for T2, based on Brazilian wet periods (Wang et al., 2004), it seems plausible that elevated proportions of *G. truncatulinoides* during T2 may serve as indication of strong sea surface winter cooling/salinification amplified by intensified atmospheric circulation intensified trade winds coupled with cold meteorological fronts enhance upper water column mixing in the region through evaporative cooling during boreal winter, when the ITCZ is at the southernmost position (e.g., Wilson and Roberts, 1995).

Deleted:

This is in contrast to the subtropical N. Atlantic where winter sea surface cooling ($T < 23^{\circ}\text{C}$) and deep mixing occur alongside with increase of *G. truncatulinoides* up to 15% (Levitus et al., 2013; Siccha and Kučera, 2017). It could, therefore, be proposed that the overall abundance of *G. truncatulinoides* in our subtropical settings was at least partly controlled by oceanic conditions occurring nearer to the sea surface (Mulitza et al., 1997; Jonkers and Kučera, 2016). [†] elevated occurrences of transitional to subpolar species *G. inflata* indicate generally cold-water conditions off the LBB.

Deleted: is

Deleted: , therefore, increased Fe content in the sediment

Deleted: the

Deleted: 5D

Deleted:

Deleted: , i.e., during colder periods

Deleted: ; Tjallingii et al., 2008

Deleted:

Deleted: Finally, increased velocities of the wind-driven

Deleted: Early

Deleted: properties (temperature, salinity, nutrients)

Deleted: i

Deleted: 6

Deleted: 5

Deleted: (between 20°N and 20°S),

and Hemleben, 2017). Therefore, fluctuations in relative abundances of *G. sacculifer* and *G. ruber* (pink) are referred here as to represent a warm “tropical” end-member (Fig. 1b). Relative abundances of the tropical foraminifera (here and further in the text *G. ruber* (pink) and *G. sacculifer* calculated together) in our core suggest an early thermal maximum (between ~129 and 124 ka), which agrees well with the recent compilation of global MIS 5e SST (Hoffman et al., 2017). The sea surface warming could be related to a northward expansion of the Atlantic Warm Pool (Ziegler et al., 2008), in response to a northern location of the mean annual position of the ITCZ. The latter shift in the atmospheric circulation is explained by the particularly strong northern hemisphere insolation during early MIS 5e (Fig. 6), resulting in a cross-latitudinal thermal gradient change, and in turn, forcing the ITCZ towards a warming (northern) hemisphere (Schneider et al., 2014). A northern location of the mean annual position of the ITCZ during the first phase of the last interglacial is supported by the XRF data from the Cariaco Basin, showing highest accumulation of the redox-sensitive element molybdenum (Mo) during early MIS 5e (Fig. 6). At that latter location, high Mo content is found in sediments deposited under anoxic conditions, occurring only during warm interstadial periods associated with a northerly shifted ITCZ (Gibson and Peterson, 2014).

Further, our data reveal a millennial-scale cooling/salinification event at ~127 ka, characterized by decreased proportions of the tropical foraminifera and elevated planktic $\delta^{18}\text{O}$ values (Fig. 6). That this abrupt cooling characterized the entire upper water column at the onset of the event is indicated by the re-occurrence of cold-water species *G. inflata* coincident with the brief positive excursions in $\delta^{18}\text{O}$ values in the shallow and thermocline-dwelling foraminifera (Fig. 4). Simultaneously, the XRF record from the Cariaco Basin reveals a stadial-like Mo-depleted (i.e., southward ITCZ shift) interval (Fig. 6). The close similarity between the tropical-species record from the Bahamas and the XRF data from the Cariaco Basin supports the hypothesis that the annual displacements of the ITCZ are also documented in our faunal counts. Thus, a southward shift in the mean annual position of the ITCZ at ~127 ka could have restricted influence of the Atlantic Warm Pool in the Bahama region, reducing SST and possibly increasing SSS, and in turn, affecting the foraminiferal assemblage. Moreover, because the aforementioned abrupt climatic shift at ~127 ka cannot be reconciled with insolation changes, other forcing factors at play during early MIS 5e should be considered. Studies from the low-latitude Atlantic reveal strong coupling between the ITCZ position and the AMOC strength associated with millennial-scale climatic variability (Rühlemann et al., 1999; Schmidt et al., 2006a; Carlson et al., 2008). In particular, model simulations and proxy data suggest that freshwater inputs as well as sea-ice extent in the (sub)polar North Atlantic can affect the ITCZ

Deleted: 1B

Deleted: ¶

As shown in Fig. 7B, relative abundances of tropical species (here and further in the text *G. ruber* (pink) and *G. sacculifer* calculated together) increased before the onset of the last interglacial “plateau” at ~129 ka. This transition was

Deleted: possibly coupled

Deleted: with

Deleted: the intensification of the Gulf Stream at MIS 6/5e boundary (Bahr et al., 2011).

Deleted: Accordingly,

Deleted: In addition, a gradual rise in

Deleted: in sediment data from Cariaco Basin is observed across the penultimate deglaciation

Deleted: 7D

Deleted: s

Deleted: 4-7

Deleted: c

Deleted: across the

Deleted: occurred

Deleted: *G. falconensis* and

Deleted: of

Deleted: deep

Deleted: A coherent cooling event, dated by U-Th to be centered around 127 ka, is also evident in an isotopic record from the southwestern slope of the LBB (Slowey et al., 1996; Henderson et al., 2000), suggesting at least a regional expression of the event.

Deleted: sediments

Deleted: southward

Deleted: 7D

Deleted: the

Deleted: additional

Deleted: . ¶

a gradual northward migration of the mean annual position of the ITCZ at the onset of MIS 5e could be implied. In line with increasing low latitude summer insolation (Fig. 7C), this ITCZ displacement would also promote a northward expansion of tropical pool waters (Ziegler et al., 2008). Because core MD99-2202 is located at the northern edge of ITCZ influence, the rapid shift in foraminiferal proportions at ~130 ka could, in fact, represent the onset of warm pool waters influence, which resulted from a gradual northward-directed ITCZ movement. Accordingly, a gradual northward migration of the mean annual position of the ITCZ at the onset of MIS 5e could be implied. In line with increasing low latitude summer insolation (Fig. 7C), this ITCZ displacement would also promote a northward expansion of tropical pool waters (Ziegler et al., 2008). Because core MD99-2202 is located at the northern edge of ITCZ influence, the rapid shift in foraminiferal proportions at ~130 ka could, in fact, represent the onset of warm pool waters influence, which resulted from a gradual northward-directed ITCZ movement. Similarly, the pronounced increase in the tropical species [25]

position through feedbacks on the thermohaline circulation and associated change in the cross-latitudinal heat redistribution (e.g., Chiang et al., 2003; Broccoli et al., 2006; Gibson and Peterson, 2014). It is well-established that the deepwater overflow from the Nordic Seas, which constitutes the deepest southward-flowing branch of the AMOC today (e.g., Stahr and Sanford, 1999), strengthened (deepened) only during the second phase of MIS 5e (at ~124 ka), and after the deglacial meltwater input into the region ceased (Hodell et al., 2009; Barker et al., 2015). Nevertheless, several studies show that the deep-water ventilation and presumably the AMOC abruptly recovered at the beginning of MIS 5e, at ~129 ka (Fig. 6), possibly linked to a deepened winter convection in the Northwestern Atlantic (Adkins et al., 1997; Galaasen et al., 2014; Deane et al., 2017). Accordingly, the resumption of the AMOC could have added to a meridional redistribution of the incoming solar heat, changing cross-latitudinal thermal gradient and, thus, contributing to the inferred “orbitally-driven” northward ITCZ shift during early MIS 5e (see above). In turn, the millennial-scale climatic reversal between 127 and 126 ka could have been related to the known reductions of deep water ventilation (Galaasen et al., 2014; Deane et al., 2017), possibly attributed to a brief increase in the freshwater input into the subpolar North Atlantic and accompanied by a regional sea surface cooling (Irvali et al., 2012; Zhuravleva et al., 2017b). A corresponding cooling and freshening event, referred here and elsewhere as to a Younger Dryas-like event, is captured in some high- and mid-latitude North Atlantic records (Sarnthein and Tiedemann, 1990; Bauch et al., 2012; Irvali et al., 2012; Schwab et al., 2013; Govin et al., 2014; Jiménez-Amat and Zahn, 2015). Coherently with the Younger Dryas-like cooling and the reduction (shallowing) in the North Atlantic Deep Water formation, an increase in the Antarctic Bottom Water influence is revealed in the Southern Ocean sediments, arguing for the existence of an “interglacial” bipolar seesaw (Hayes et al., 2014). The out-of-phase climatic relationship between high northern and high southern latitudes, typical for the last glacial termination (Barker et al., 2009), could be attributed to a strong sensitivity of the transitional climatic regime of early MIS 5e due to persistent high-latitude freshening (continuing deglaciation, Fig. 6) and suppressed overturning in the Nordic Seas (Hodell et al., 2009). This assumption seems of crucial importance as it might help explain a relatively “late” occurrence of the Younger Dryas-like event during the last interglacial, when compared to the actual Younger Dryas during the last deglaciation (Bauch et al., 2012). The recognition of the transitional phase during early MIS 5e is not new, but only few authors have pointed out its importance for understanding the last interglacial climatic evolution beyond the subpolar regions (e.g., Govin et al., 2012; Schwab et al., 2013; Kandiano et al., 2014). As insolation forcing decreased during late MIS 5e and the ITCZ gradually moved southward, the white variety of *G. ruber* started to dominate the assemblage (Fig. 5), arguing for generally colder sea surface conditions in the

- Deleted: ¶
- Deleted:
- Deleted: s
- Deleted: ing
- Deleted: today
- Deleted: ¶
- Although the full resumption of the AMOC from a shallow or weak mode during T2 occurred only by ~124 ka,
- Deleted: apparently
- Deleted: due
- Deleted: Labrador Sea
- Deleted: In accordance with previous studies from the tropical N. Atlantic suggesting a coupling between ITCZ position and ocean overturning (Rühlemann et al., 1999; Schmidt et al., 2006a; Carlson et al., 2008), it could be argued
- Deleted: during early MIS 5e
- Deleted: –
- Deleted: elsewhere
- Deleted: type
- Deleted: -
- Deleted: .
- Deleted: 1????
- Deleted: ; Zhuravleva et al., 2017a
- Deleted: type
- Deleted: /shallowing
- Deleted: NADW
- Deleted: formation
- Deleted:
- Deleted: core data
- Deleted: is
- Deleted: t
- Deleted: because
- Deleted: it
- Deleted: s
- Deleted: to
- Deleted: such
- Deleted: type
- Deleted: T2
- Deleted: ,
- Deleted: in
- Deleted: several
- Deleted: ¶ ... [27]
- Deleted: the
- Deleted: (Fig. 7C-D)
- Deleted: 6

1169 Bahama region. The inferred broad salinity tolerance of this species, also to neritic conditions (Bé and Tolderlund,
 1170 1971; Schmuker and Schiebel, 2002), was used in some studies to link high proportions of *G. ruber* (pink and
 1171 white varieties) with low SSS (Vautravers et al., 2007; Kandiano et al., 2012). The plots of the global distribution
 1172 pattern of *G. ruber* (white) and *G. ruber* (pink), however, suggest that when relative abundances of these two
 1173 species are approaching maximum values (40% and 10%, respectively), the SSSs would be higher for specimens
 1174 of the white variety of *G. ruber* (Hilbrecht, 1996). Therefore, the strongly dominating white versus pink *G. ruber*
 1175 variety observed in our records during late MIS 5e could be linked not only to decreasing SSTs, but also to
 1176 increasing SSSs.

1177 In their study from the western STG, Bahr et al. (2013) also reconstruct sea surface salinification during late MIS
 1178 5e in response to enhanced wind stress at times of deteriorating high-latitude climate and increasing meridional
 1179 gradients. Accordingly, our isotopic and faunal data (note the abrupt decrease in *G. sacculifer* proportion at 120
 1180 ka; Fig. 5) suggest a pronounced climatic shift that could be attributed to the so-called “neoglaciation”, consistent
 1181 with the sea surface cooling in the western Nordic Seas and the Labrador Sea (Van Nieuwenhove et al., 2013;
 1182 Irvani et al., 2016) as well as with a renewed growth of terrestrial ice (Fronval and Jansen, 1997; Zhuravleva et
 1183 al., 2017a).

1184 7 Conclusions

1185 New faunal, isotopic, and XRF evidence from the Bahama region were studied for past subtropical climatic
 1186 evolution, with special attention given to (a) the mechanisms controlling the planktic foraminiferal assemblage
 1187 and (b) the climatic feedbacks between low and high latitudes.

1188 During late MIS 6 and glacial termination, strongly reduced $\delta^{18}\text{O}$ gradients between surface and thermocline-
 1189 dwelling foraminifera suggest decreased water column stratification, which promoted high relative abundances
 1190 of *G. truncatulinoides* (dex) and *G. inflata*. The lowered upper water column stratification, in turn, could be a
 1191 result of sea surface cooling/salinification and intensified trade winds strength at times of the ITCZ being shifted
 1192 far to the south.

1193 Computed together, relative abundances of the tropical foraminifera *G. sacculifer* and *G. ruber* (pink) agree well
 1194 with the published ITCZ-related Cariaco Basin record (Gibson and Peterson, 2014), suggesting a climatic
 1195 coupling between the regions. Based on these data, a northward/southward displacement of the mean annual ITCZ
 1196 position, in line with strong/weak northern hemisphere insolation, could be inferred for early/late MIS 5e.
 1197 Crucially, an abrupt Younger Dryas-like sea surface cooling/salinification event at ~127 ka intersected the early
 1198 MIS 5e warmth (between ~129 and 124 ka) and could be associated with a sudden southward displacement of the

Deleted: surface salinities

Deleted: the sea surface salinities

Deleted: s.

Deleted: SST

Deleted: sea surface salinity

Deleted: 6B

Deleted: a

Deleted: 2017b

Deleted: Notably, a small but coherent increase in the aragonite content and Sr counts is evident at 120 ka and coincides with the change towards finer-grained sediments, altogether arguing for a change in sedimentary regime before the end of the major flooding interval at ~117 ka (Figs. 2 and 4). Further interpretations of the aragonite changes based on the available data appear rather speculative, given that the aragonite precipitation on the platform top at times of sea level highstand is controlled by level of aragonite supersaturation, which, in turn, depends on a number of climate-related parameters, such as CO₂ amounts, temperature, salinity, water depth above the bank top as well as residence time of the water mass above the platform (Morse and Mackenzie, 1990; Morse and He, 1993; Roth and Reijmer, 2004; 2005). Nevertheless, the coherent shift in the carbonate mineralogy revealed after 120 ka may support major oceanographic and atmospheric changes during the late phase of MIS 5e possibly coupled with a significant sea level change.

Deleted: , faunal

Deleted: combined with published sedimentological data from a sediment core obtained from the slope of the LBB

Deleted: changes in water masses, sedimentary regimes, and RSL change across the last interglacial. By using new data, we were able to better constrain the last interglacial cycle in the investigated core section (cf. Lantzsich et al., [28])

Deleted: 2:

Deleted: S

Deleted: mixed-layer

Deleted: r

Deleted: . H

Deleted: proportions

Deleted: c

Deleted: attributed

Deleted: to a deep winter mixing as

Deleted: winter

Deleted: depressed

Deleted: ¶

Deleted: Early MIS 5e:

Deleted: forcing

Deleted: However

Deleted: event

Deleted: (give age!!!)

ITCZ. This atmospheric shift, could be, in turn, related to a millennial-scale instability in the ocean overturning, supporting a cross-latitudinal teleconnection that influenced the subtropical climate via ocean-atmospheric forcing. These observations lead to an inference that the persistent ocean freshening in the high northern latitudes (i.e., continuing deglaciation) and, therefore, unstable deep water overturning during early MIS 5e accounted for a particularly sensitive climatic regime, associated with the abrupt warm-cold switches that could be traced across various oceanic basins.

Data availability

All data will be made available in the online database PANGAEA (www.pangaea.de).

Acknowledgments

We wish to thank H. Lantzsch and J. J. G. Reijmer for providing us with the sediment core and data from core MD99-2202, S. Fessler for performing measurements on stable isotopes, S. Müller and D. Garbe-Schönberg for technical assistance during XRF scanning, J. Lübbers for her help with sample preparation, and E. Kandiano for introduction into tropical foraminiferal assemblages. Comments by A. Bahr and one anonymous reviewer greatly improved the manuscript. A. Z. acknowledges funding from German Research Foundation (DFG grant BA1367/12-1).

References

- Adkins, J. F., Boyle, E. A., Keigwin, L. and Cortijo, E.: Variability of the North Atlantic thermohaline circulation during the last interglacial period, *Nature*, 390, 154, doi:10.1038/36540, 1997.
- Arbuszewski, J. A., deMenocal, P. B., Cléroux, C., Bradtmiller, L., Mix, A.: Meridional shifts of the Atlantic intertropical convergence zone since the Last Glacial Maximum, *Nature Geosci.* 6, 959, doi:10.1038/ngeo1961, 2013.
- Bahr, A., Nürnberg, D., Schönfeld, J., Garbe-Schönberg, D.: Hydrological variability in Florida Straits during Marine Isotope Stage 5 cold events, *Paleoceanography*, 26, doi:10.1029/2010PA002015, 2011.
- Bahr, A., Nürnberg, D., Karas, C. and Grützner, J.: Millennial-scale versus long-term dynamics in the surface and subsurface of the western North Atlantic Subtropical Gyre during Marine Isotope Stage 5, *Glob. Planet. Change*, 111, 77–87, doi:10.1016/j.gloplacha.2013.08.013, 2013.

Deleted:

This so-called Younger Dryas type cooling event likely involved AMOC-related forcing that influenced (sub)tropical climate. The relatively late occurrence of Younger Dryas type cooling event, when compared to the actual Younger Dryas in the last deglaciation, is attributed to the transitional climatic regime of early MIS 5e, characterized by persistent high-latitude freshening and unstable deep-water overturning in the N. Atlantic.

Late MIS 5e: Overall sea surface cooling and possibly salinification is reconstructed for the Bahama region, in accordance with insolation decrease and a gradual southward displacement of the mean annual ITCZ. A coherent change is observed in faunal, isotopic and sedimentological proxies, arguing for coupled oceanic and northern hemisphere cryospheric reorganizations before the end of the major flooding period.

Deleted: Comments by A. Bahr and one anonymous reviewer greatly improved the manuscript.

Deleted:

Deleted: .

Deleted: .

Deleted:

1325 Bahr, A., Jiménez-Espejo, F. J., Kolasinac, N., Grunert, P., Hernández-Molina F. J., Röhl U., Voelker A. H. L.,
 1326 Escutia C., Stow D. A. V., Hodel D. and Alvarez-Zarikian C. A.: Deciphering bottom current velocity
 1327 and paleoclimate signals from contourite deposits in the Gulf of Cádiz during the last 140 kyr: An
 1328 inorganic geochemical approach, *Geochem. Geophys. Geosyst.*, 15, 3145–3160,
 1329 doi:10.1002/2014GC005356, 2014.
 1330 Barker, S., Diz, P., Vautravers, M. J., Pike, J., Knorr, G., Hall, I. R. and Broecker, W. S.: Interhemispheric Atlantic
 1331 seesaw response during the last deglaciation, *Nature*, 457, 1097, doi:10.1038/nature07770, 2009.
 1332 [Barker, S., Chen, J., Gong, X., Jonkers, L., Knorr, G., Thornalley, D.: Icebergs not the trigger for North Atlantic](#)
 1333 [cold events, *Nature* 520, 333, doi: 10.1038/nature14330, 2015.](#)
 1334 [Bauch, H. A., Kandiano, E. S. and Helmke, J. P.: Contrasting ocean changes between the subpolar and polar North](#)
 1335 [Atlantic during the past 135 ka, *Geophys. Res. Lett.*, 39, doi:10.1029/2012GL051800, 2012.](#)
 1336 Bé, A. W. H. and Tolderlund, D. S.: Distribution and ecology of living planktonic foraminifera in surface waters
 1337 of the Atlantic and Indian Oceans, in: Funnell, B. and Riedel, W.R. (Eds.), *The Micropalaeontology of*
 1338 *Oceans*, Cambridge University Press, Cambridge, pp. 105–149, 1971.
 1339 Boli, H. M. and Saunders, J. B.: Oligocene to Holocene low latitude planktic foraminifera, in: Bolli, H.M.,
 1340 Saunders, J.B., Perch-Nielsen, K. (Eds.), *Plankton Stratigraphy*, Cambridge University Press, New York,
 1341 pp. 155–262, 1985.
 1342 [Broccoli, A. J., Dahl, K. A., Stouffer, R. J.: Response of the ITCZ to Northern Hemisphere cooling, *Geophys.*
 1343 \[Res. Lett.\]\(#\) 33, doi:10.1029/2005GL024546, 2006.](#)
 1344 [Carew, J. L. and Mylroie, J. E.: Quaternary tectonic stability of the Bahamian archipelago: evidence from fossil](#)
 1345 [coral reefs and flank margin caves, *Quat. Sci. Rev.*, 14, 145–153, doi:10.1016/0277-3791\(94\)00108-N,](#)
 1346 [1995.](#)
 1347 Carew, J. L. and Mylroie, J. E.: Geology of the Bahamas, in: *Geology and Hydrogeology of Carbonate Islands,*
 1348 *Developments in Sedimentology*, 54, Elsevier Science, pp. 91–139, 1997.
 1349 Carlson, A. E., Oppo, D. W., Came, R. E., LeGrande, A. N., Keigwin, L. D. and Curry, W. B.: Subtropical Atlantic
 1350 salinity variability and Atlantic meridional circulation during the last deglaciation, *Geology*, 991–994,
 1351 doi:10.1130/G25080A, 2008.
 1352 [Chabaud, L.: Modèle stratigraphique et processus sédimentaires au Quaternaire sur deux pentes carbonatées des](#)
 1353 [Bahamas \(leeward et windward\), Doctoral dissertation, Université de Bordeaux, Français, 2016.](#)

Deleted: ¶

Deleted: ¶

1356 Chabaud, L., Ducassou, E., Tournadour, E., Mulder, T., Reijmer, J. J. G., Conesa, G., Giraudeau, J., Hanquiez,
 1357 V., Borgomano, J. and Ross, L.: Sedimentary processes determining the modern carbonate periplatform
 1358 drift of Little Bahama Bank, *Mar. Geol.*, 378, 213–229, doi:10.1016/j.margeo.2015.11.006, 2016.
 1359 [Chang, P., Zhang, R., Hazeleger, W., Wen, C., Wan, X., Ji, L., Haarsma, R. J., Breugem, W.-P., Seidel, H.:](#)
 1360 [Oceanic link between abrupt changes in the North Atlantic Ocean and the African monsoon, *Nat.*](#)
 1361 [Geosci.](#), 1, 444, doi:10.1038/ngeo218, 2008.
 1362 [Chiang, J. C. H., Biasutti, M., Battisti, D.S.: Sensitivity of the Atlantic Intertropical Convergence Zone to Last](#)
 1363 [Glacial Maximum boundary conditions, *Paleoceanography*, 18, doi:10.1029/2003PA000916, 2003.](#)
 1364 [Chiang, J. C. H., Cheng, W., Bitz, C.M.: Fast teleconnections to the tropical Atlantic sector from Atlantic](#)
 1365 [thermohaline adjustment, *Geophys. Res. Lett.*, 35, doi:10.1029/2008GL033292, 2008.](#)
 1366 Cléroux, C., Cortijo, E., Duplessy, J. and Zahn, R.: Deep-dwelling foraminifera as thermocline temperature
 1367 recorders, *Geochem. Geophys. Geosyst.*, 8(4), doi:10.1029/2006GC001474, 2007.
 1368 Cortijo, E., Lehman, S., Keigwin, L., Chapman, M., Paillard, D. and Labeyrie, L.: Changes in Meridional
 1369 Temperature and Salinity Gradients in the North Atlantic Ocean (30°–72°N) during the Last Interglacial
 1370 Period, *Paleoceanography*, 14, 23–33, doi:10.1029/1998PA900004, 1999.
 1371 Deaney, E. L., Barker, S. and van de Flierdt, T.: Timing and nature of AMOC recovery across Termination 2 and
 1372 magnitude of deglacial CO₂ change, *Nat. Commun.*, 8, 14595, doi:10.1038/ncomms14595, 2017.
 1373 [Droxler, A. W. and Schlager, W.: Glacial versus interglacial sedimentation rates and turbidite frequency in the](#)
 1374 [Bahamas, *Geology* 13, 799–802, 1985.](#)
 1375 [Dutton, A., Carlson, A. E., Long, A. J., Milne, G. A., Clark, P. U., DeConto, R., Horton, B. P., Rahmstorf, S. and](#)
 1376 [Raymo, M. E.: Sea-level rise due to polar ice-sheet mass loss during past warm periods, *Science*, 349,](#)
 1377 [doi:10.1126/science.aaa4019, 2015.](#)
 1378 Ericson, D. B. and Wollin, G.: Pleistocene climates and chronology in deep-sea sediments, *Science*, 162(3859),
 1379 1227–1234, 1968.
 1380 Fronval, T. and Jansen, E.: Eemian and Early Weichselian (140–60 ka) Paleoceanography and paleoclimate in the
 1381 Nordic Seas with comparisons to Holocene conditions, *Paleoceanography*, 12, 443–462,
 1382 doi:10.1029/97PA00322, 1997.
 1383 Galaasen, E. V., Ninnemann, U. S., Irvahl, N., Kleiven, H. (Kikki) F., Rosenthal, Y., Kissel, C. and Hodell, D. A.:
 1384 Rapid Reductions in North Atlantic Deep Water During the Peak of the Last Interglacial Period, *Science*,
 1385 343, 1129, doi:10.1126/science.1248667, 2014.


Deleted: Chabaud, L.: Modèle stratigraphique et
 processus sédimentaires au Quaternaire sur deux pentes
 carbonatées des Bahamas (leeward et windward),
 Stratigraphie. Université de Bordeaux, Français, 2016.

Deleted:

Deleted:


1392 Gibson, K. A. and Peterson, L. C.: A 0.6 million year record of millennial-scale climate variability in the tropics,
 1393 Geophys. Res. Lett., 41, 969–975, doi:10.1002/2013GL058846, 2014.
 1394 Govin, A., Braconnot, P., Capron, E., Cortijo, E., Duplessy, J.-C., Jansen, E., Labeyrie, L., Landais, A., Marti, O.,
 1395 Michel, E., Mosquet, E., Risebrobakken, B., Swingedouw, D. and Waelbroeck, C.: Persistent influence
 1396 of ice sheet melting on high northern latitude climate during the early Last Interglacial, Clim. Past, 8,
 1397 483–507, doi:10.5194/cp-8-483-2012, 2012.
 1398 Govin, A., Varma, V. and Prange, M.: Astronomically forced variations in western African rainfall (21°N–20°S)
 1399 during the Last Interglacial period, Geophys. Res. Lett., 41, 2117–2125, doi:10.1002/2013GL058999,
 1400 2014.
 1401 Govin, A., Capron, E., Tzedakis, P. C., Verheyden, S., Ghaleb, B., Hillaire-Marcel, C., St-Onge, G., Stoner, J. S.,
 1402 Bassinot, F., Bazin, L., Blunier, T., Combourieu-Nebout, N., El Ouahabi, A., Genty, D., Gersonde, R.,
 1403 Jiménez-Amat, P., Landais, A., Martrat, B., Masson-Delmotte, V., Parrenin, F., Seidenkrantz, M.-S.,
 1404 Veres, D., Waelbroeck, C. and Zahn, R.: Sequence of events from the onset to the demise of the Last
 1405 Interglacial: Evaluating strengths and limitations of chronologies used in climatic archives, Quat. Sci.
 1406 Rev., 129, 1–36, doi:10.1016/j.quascirev.2015.09.018, 2015.
 1407 Grant, K. M., Rohling, E. J., Bar-Matthews, M., Ayalon, A., Medina-Elizalde, M., Ramsey, C. B., Satow, C. and
 1408 Roberts, A. P.: Rapid coupling between ice volume and polar temperature over the past 150,000 years,
 1409 Nature, 491, 744, doi:10.1038/nature11593, 2012.
 1410 Groeneveld, J. and Chiessi, C. M.: Mg/Ca of *Globorotalia inflata* as a recorder of permanent thermocline
 1411 temperatures in the South Atlantic, Paleoceanography, 26, doi:10.1029/2010PA001940, 2011.
 1412 Hayes, C. T., Martínez-García, A., Hasenfratz, A. P., Jaccard, S. L., Hodell, D. A., Sigman, D. M., Haug, G. H.
 1413 and Anderson, R. F.: A stagnation event in the deep South Atlantic during the last interglacial period,
 1414 Science, 346, 1514–1517, doi:10.1126/science.1256620, 2014.
 1415 Hearty, P. J. and Neumann, A. C.: Rapid sea level and climate change at the close of the Last Interglaciation (MIS
 1416 5e): evidence from the Bahama Islands, Quat. Sci. Rev., 20, 1881–1895, doi:10.1016/S0277-
 1417 3791(01)00021-X, 2001.
 1418 Hearty, P. J., Hollin, J. T., Neumann, A. C., O’Leary, M. J. and McCulloch, M.: Global sea-level fluctuations
 1419 during the Last Interglaciation (MIS 5e), Quat. Sci. Rev., 26, 2090–2112, doi:
 1420 10.1016/j.quascirev.2007.06.019, 2007.

1421 Helmke, J. P., Bauch, H. A., Röhl, U. and Kandiano, E. S.: Uniform climate development between the subtropical
 1422 and subpolar Northeast Atlantic across marine isotope stage 11, *Clim. Past*, 4, 181–190, doi:10.5194/cp-
 1423 4-181-2008, 2008.

1424  Hennekam, R. and de Lange, G.: X-ray fluorescence core scanning of wet marine sediments: methods to improve
 1425 quality and reproducibility of high-resolution paleoenvironmental records, *Limnol. Oceanogr.*, 10, 991–
 1426 1003, doi:10.4319/lom.2012.10.991, 2012.

1427 Hilbrecht, H.: Extant planktic foraminifera and the physical environment in the Atlantic and Indian Oceans: an
 1428 atlas based on Climap and Levitus (1982) data. *Mitteilungen aus dem Geologischen Institut der Eidgen.
 1429 Technischen Hochschule und der Universität Zürich, Neue Folge*, Zürich, 93 pp, 1996.


1430 Hodell, D. A., Minth, E. K., Curtis, J. H., McCave, I. N., Hall, I. R., Channell, J. E. T., Xuan, C.: Surface and
 1431 deep-water hydrography on Gardar Drift (Iceland Basin) during the last interglacial period, *Earth Planet.*
 1432 *Sci. Lett.*, 288, 10–19, doi:10.1016/j.epsl.2009.08.040, 2009.

1433  Hoffman, J. S., Clark, P. U., Parnell, A. C. and He, F.: Regional and global sea-surface temperatures during the
 1434 last interglaciation, *Science*, 355, 276, doi:10.1126/science.aai8464, 2017.



1435 Irvali, N., Ninnemann, U. S., Galaasen, E. V., Rosenthal, Y., Kroon, D., Oppo, D. W., Kleiven, H. F., Darling, K.
 1436 F. and Kissel, C.: Rapid switches in subpolar North Atlantic hydrography and climate during the Last
 1437 Interglacial (MIS 5e), *Paleoceanography*, 27, PA2207, doi:10.1029/2011PA002244, 2012.

1438 Irvali, N., Ninnemann, U. S., Kleiven, H. (Kikki) F., Galaasen, E. V., Morley, A. and Rosenthal, Y.: Evidence for
 1439 regional cooling, frontal advances, and East Greenland Ice Sheet changes during the demise of the last
 1440 interglacial, *Quat. Sci. Rev.*, 150, 184–199, doi:10.1016/j.quascirev.2016.08.029, 2016.

1441 Jentzen, A., Schönfeld, J., Schiebel, R.: Assessment of the Effect of Increasing Temperature On the Ecology and
 1442 Assemblage Structure of Modern Planktic Foraminifers in the Caribbean and Surrounding Seas, *J.*
 1443 *Foraminiferal Res.* 251–272, doi: 10.2113/gsjfr.48.3.251, 2018.

1444  Jiménez-Amat, P. and Zahn, R.: Offset timing of climate oscillations during the last two glacial-interglacial
 1445 transitions connected with large-scale freshwater perturbation, *Paleoceanography*, 30, 768–788,
 1446 doi:10.1002/2014PA002710, 2015.

1447 Johns, W. E., Townsend, T. L., Frantoni, D. M. and Wilson, W. D.: On the Atlantic inflow to the Caribbean
 1448 Sea. Deep Sea Research Part I: Oceanogr. Res. Pap., 49, 211–243. doi:10.1016/S0967-0637(01)00041-
 1449 3. 2002.

Deleted: Henderson, G. M. and Slowey, N. C.: Evidence from U–Th dating against Northern Hemisphere forcing of the penultimate deglaciation, *Nature*, 404, 61, doi:10.1038/35003541, 2000. 
 Henderson, G. M., Rendle, R. H., Slowey, N. C., and Reijmer, J. J. G.: U–Th dating and diagenesis of Pleistocene highstand sediments from the Bahamas slope, *Ocean Drilling Program, Scientific Results*, 166, 61–76, 2000. 

Deleted: 

Deleted: 

1461 Jonkers, L. and Kučera, M.: Global analysis of seasonality in the shell flux of extant planktonic Foraminifera,
 1462 Biogeosci., 12, 2207–2226, doi:10.5194/bg-12-2207-2015, 2015.

1463 Kandiano, E. S., Bauch, H. A., Fahl, K., Helmke, J. P., Röhl, U., Pérez-Folgado, M. and Cacho, I.: The meridional
 1464 temperature gradient in the eastern North Atlantic during MIS 11 and its link to the ocean–atmosphere
 1465 system, Palaeogeogr. Palaeoclimatol. Palaeoecol., 333–334, 24–39, doi:10.1016/j.palaeo.2012.03.005,
 1466 2012.

1467 [Kandiano, E. S., Bauch, H. A., Fahl, K., 2014. Last interglacial surface water structure in the western](#)
 1468 [Mediterranean \(Balearic\) Sea: Climatic variability and link between low and high latitudes, Glob. Planet.](#)
 1469 [Change, 123, 67–76, doi:10.1016/j.gloplacha.2014.10.004, 2014.](#)

1470 [Kopp, R. E., Simons, F. J., Mitrovica, J. X., Maloof, A. C. and Oppenheimer, M.: Probabilistic assessment of sea](#)
 1471 [level during the last interglacial stage, Nature, 462, 863–867, doi:10.1038/nature08686, 2009.](#)

1472 [Lantzsich, H., Roth, S., Reijmer, J. J. G. and Kinkel, H.: Sea-level related resedimentation processes on the](#)
 1473 [northern slope of Little Bahama Bank \(Middle Pleistocene to Holocene\), Sedimentology, 54, 1307–1322,](#)
 1474 [doi:10.1111/j.1365-3091.2007.00882.x, 2007.](#)

1475 Laskar, J., Robutel, P., Joutel, F., Gastineau, M., Correia, A. C. M. and Levrard, B.: A long-term numerical
 1476 solution for the insolation quantities of the Earth, Astron. Astrophys., 428, 261–285, doi:10.1051/0004-
 1477 6361:20041335, 2004.

1478 Levitus, S., Antonov, J. I., Baranova, O. K., Boyer, T. P., Coleman, C. L., Garcia, H. E., Grodsky, A. I., Johnson,
 1479 D. R., Locarnini, R. A. and Mishonov, A. V.: The world ocean database, Data Sci. J., 12, WDS229-
 1480 WDS234, 2013.

1481 Lisiecki, L. E. and Stern, J. V.: Regional and global benthic $\delta^{18}\text{O}$ stacks for the last glacial cycle,
 1482 Paleoceanography, 31, 1368–1394, doi:10.1002/2016PA003002, 2016.

1483 Lohmann, G. P. and Schweitzer, P. N.: Globorotalia truncatulinoides' Growth and chemistry as probes of the past
 1484 thermocline: 1. Shell size, Paleoceanography, 5, 55–75, doi:10.1029/PA005i001p00055, 2010.

1485 Loulergue, L., Schilt, A., Spahni, R., Masson-Delmotte, V., Blunier, T., Lemieux, B., Barnola, J.-M., Raynaud,
 1486 D., Stocker, T. F. and Chappellaz, J.: Orbital and millennial-scale features of atmospheric CH_4 over the
 1487 past 800,000 years, Nature, 453, 383–386, doi:10.1038/nature06950, 2008.

1488 Masson-Delmotte, V., Schulz, M., Abe-Ouchi, A., Beer, J., Ganopolski, A., González Rouco, J. F., Jansen, E.,
 1489 Lambeck, K., Luterbacher, J. and Naish, T.: Information from paleoclimate archives, in: Stocker, T. F.,
 1490 Qin, D., Plattner, G.-K., Tignor, M., Allen, S. K., Boschung, J., Nauels, A., Xia, Y., Bex, V., Midgley,

Deleted: ¶

Deleted: Labeyrie, L. D. and Reijmer, J. J. G.: Physical properties of sediment core MD99-2202. doi:10.1594/PANGAEA.253089, 2005.¶

1495 P.M. (Eds.), Climate Change 2013: The Physical Science Basis. Contribution of Working Group I to the
 1496 Fifth Assessment Report of the Intergovernmental Panel on Climate Change, pp. 383–464, 2013.

1497 ~~Morse, J. W. and MacKenzie, F. T.: Geochemistry of sedimentary carbonates, Elsevier, 1990.~~
 1498 Muhs, D. R., Budahn, J. R., Prospero, J. M., Carey, S. N.: Geochemical evidence for African dust inputs to soils
 1499 of western Atlantic islands: Barbados, the Bahamas, and Florida, J. Geophys. Res.: Earth Surface, 112,
 1500 doi:10.1029/2005JF0004452007, 2007.

1501 ~~Mulitza, S., Dürkoop, A., Hale, W., Wefer, G. and Niebler, H. S.: Planktonic foraminifera as recorders of past~~
 1502 ~~surface-water stratification, Geology, 25(4), 335–338, doi:10.1130/0091-~~
 1503 ~~7613(1997)025<0335:PFAROP>2.3.CO;2, 1997.~~

1504 Neumann, A. C. and Land, L. S.: Lime mud deposition and calcareous algae in the Bight of Abaco, Bahamas; a
 1505 budget, J. Sediment. Res., 45, 763–786, 1975.

1506 ~~NGRIP community members: High-resolution record of Northern Hemisphere climate extending into the last~~
 1507 ~~interglacial period, Nature, 431, 147–151, doi:10.1038/nature02805, 2004.~~

1508 ~~Paillard, D., Labeyrie, L. and Yiou, P.: Macintosh Program performs time-series analysis, Eos Trans, AGU 77,~~
 1509 ~~379–379, doi:10.1029/96EO00259, 1996.~~

1510 Peterson, L. C. and Haug, G. H.: Variability in the mean latitude of the Atlantic Intertropical Convergence Zone
 1511 as recorded by riverine input of sediments to the Cariaco Basin (Venezuela), Palaeogeogr.
 1512 Palaeoclimatol. Palaeoecol. 234, 97–113, doi:10.1016/j.palaeo.2005.10.021, 2006.

1513 ~~Poore, R. Z., Dowsett, H. J., Verardo, S., and Quinn, T. M.: Millennial- to century-scale variability in Gulf of~~
 1514 ~~Mexico Holocene climate records, Paleoceanography, 18, doi:10.1029/2002PA000868, 2003.~~

1515 Richter, T. O., van der Gaast, S., Koster, B., Vaars, A., Gieles, R., de Stigter, H. C., De Haas, H. and van Weering,
 1516 T. C. E.: The Avaatech XRF Core Scanner: technical description and applications to NE Atlantic
 1517 sediments, Geol. Soc. London, Special Publications, 267, 39, doi:10.1144/GSL.SP.2006.267.01.03,
 1518 2006.

1519 Roth, S. and Reijmer, J. J. G.: Holocene Atlantic climate variations deduced from carbonate periplatform
 1520 sediments (leeward margin, Great Bahama Bank), Paleoceanography, 19, PA1003,
 1521 doi:10.1029/2003PA000885, 2004.

1522 Roth, S. and Reijmer, J. J. G.: Holocene millennial to centennial carbonate cyclicity recorded in slope sediments
 1523 of the Great Bahama Bank and its climatic implications, Sedimentology, 52, 161–181,
 1524 doi:10.1111/j.1365-3091.2004.00684.x, 2005.

Deleted: Morse, J. W. and He, S.: Influences of T, S and PCO₂ on the pseudo-homogeneous precipitation of CaCO₃ from seawater: implications for whiting formation, Mar. Chem., 41, 291–297, doi:10.1016/0304-4203(93)90261-L, 1993.

Deleted: Mackenzie

Deleted:

Deleted: Neumann, A. C. and Moore, W. S.: Sea Level Events and Pleistocene Coral Ages in the Northern Bahamas, Quat. Res., 5, 215–224, doi:10.1016/0033-5894(75)90024-1, 1975.

Deleted: O'Leary, M. J., Hearty, P. J., Thompson, W. G., Raymo, M. E., Mitrovica, J. X. and Webster, J. M.: Ice sheet collapse following a prolonged period of stable sea level during the last interglacial, Nature Geosci., 6, 796, doi:10.1038/ngeo1890, 2013.

Deleted:

1543 Rühlemann, C., Mulitza, S., Müller, P. J., Wefer, G. and Zahn, R.: Warming of the tropical Atlantic Ocean and
 1544 slowdown of thermohaline circulation during the last deglaciation, *Nature*, 402, 511,
 1545 doi:10.1038/990069, 1999.

1546 [Sarnthein, M. and Tiedemann, R.: Younger Dryas-style cooling events at glacial terminations I-VI at ODP site](#)
 1547 [658: Associated benthic \$\delta^{13}\text{C}\$ anomalies constrain meltwater hypothesis. *Paleoceanography and*
 1548 \[Paleoclimatology\]\(#\), 5, 1041-1055, doi: 10.1029/PA005i006p01041, 1990.](#)

1549 [Schiebel, R. and Hemleben, C.: Planktic Foraminifers in the Modern Ocean](#), Springer, 2017.

1550 Schlager, W., Reijmer, J. J. G. and Droxler, A.: Highstand Shedding of Carbonate Platforms, *J. Sedim. Res.*, 64B,
 1551 270–281, 1994.

1552 Schlitzer, R.: Ocean data view, edited, 2012.

1553 Schmidt, M. W., Vautravers, M. J. and Spero, H. J.: Rapid subtropical North Atlantic salinity oscillations across
 1554 Dansgaard–Oeschger cycles, *Nature*, 443, 561, doi:10.1038/nature05121, 2006a.

1555 Schmidt, M. W., Vautravers, M. J. and Spero, H. J.: Western Caribbean sea surface temperatures during the late
 1556 Quaternary, *Geochem. Geophys. Geosyst.*, 7, doi:10.1029/2005GC000957, 2006b.

1557 Schmitz, W. J. and McCartney, M. S.: On the North Atlantic Circulation, *Rev. Geophys.*, 31, 29–49,
 1558 doi:10.1029/92RG02583, 1993.

1559 Schmitz, W. J. and Richardson, P. L.: On the sources of the Florida Current. *Deep Sea Res. Part A: Oceanogr.*
 1560 *Res. Pap.*, 38, S379–S409, doi:10.1016/S0198-0149(12)80018-5, 1991.

1561 Schmuker, B. and Schiebel, R.: Planktic foraminifers and hydrography of the eastern and northern Caribbean Sea,
 1562 *Mar. Micropal.*, 46, 387–403, doi:10.1016/S0377-8398(02)00082-8, 2002.

1563 [Schneider, T., Bischoff, T., Haug, G. H.: Migrations and dynamics of the intertropical convergence zone, *Nature*,](#)
 1564 [513, 45, doi: 10.1038/nature13636, 2014.](#)

1565 [Schwab, C., Kinkel, H., Weinelt, M. and Repschläger, J.: A coccolithophore based view on paleoenvironmental](#)
 1566 [changes in the open ocean mid-latitude North Atlantic between 130 and 48 ka BP with special emphasis](#)
 1567 [on MIS 5e, *Quat. Sci. Rev.*, 81, 35–47, doi:10.1016/j.quascirev.2013.09.021, 2013.](#)

1568 Siccha, M. and Kučera, M.: ForCenS, a curated database of planktonic foraminifera census counts in marine
 1569 surface sediment samples, *Sci. Data*, 4, 170109, 2017.

1570 Slowey, N. C. and Curry, W. B.: Glacial-interglacial differences in circulation and carbon cycling within the upper
 1571 western North Atlantic, *Paleoceanography*, 10, 715–732, doi:10.1029/95PA01166, 1995.

Deleted: ¶

Deleted: 2010

Deleted: ¶

1575 [Slowey, N. C., Wilber, R. J., Haddad, G. A. and Henderson, G. M.: Glacial-to-Holocene sedimentation on the](#)
1576 [western slope of Great Bahama Bank, Mar. Geol., 185, 165–176, doi:10.1016/S0025-3227\(01\)00295-X,](#)
1577 [2002.](#)

1578 [Stahr, F. R. and Sanford, T. B.: Transport and bottom boundary layer observations of the North Atlantic Deep](#)
1579 [Western Boundary Current at the Blake Outer Ridge, Deep Sea Res. Part II: Topical Studies in](#)
1580 [Oceanography 46, 205–243, doi:10.1016/S0967-0645\(98\)00101-5, 1999.](#)

1581 [Stirling, C., Esat, T., Lambeck, K., McCulloch, M.: Timing and duration of the Last Interglacial: evidence for a](#)
1582 [restricted interval of widespread coral reef growth, Earth Planet. Sci. Lett., 160, 745–762,](#)
1583 [doi:10.1016/S0012-821X\(98\)00125-3, 1998.](#)

1584 [Stramma, L. and Schott, F.: The mean flow field of the tropical Atlantic Ocean. Deep Sea Res. Part II: Trop. Stud.,](#)
1585 [Oceanogr., 46, 279–303, doi:10.1016/S0967-0645\(98\)00109-X, 1999.](#)

1586 [Tjallingii, R., Röhl, U., Kölling, M. and Bickert, T.: Influence of the water content on X-ray fluorescence core-](#)
1587 [scanning measurements in soft marine sediments, Geochem. Geophys. Geosyst., 8,](#)
1588 [doi:10.1029/2006GC001393, 2007.](#)

1589 [Van Nieuwenhove, N., Bauch, H. A. and Andruleit, H.: Multiproxy fossil comparison reveals contrasting surface](#)
1590 [ocean conditions in the western Iceland Sea for the last two interglacials, Palaeogeogr. Palaeoclimatol.](#)
1591 [Palaeoecol., 370, 247–259, doi:10.1016/j.palaeo.2012.12.018, 2013.](#)

1592 [Vautravers, M. J., Shackleton, N. J., Lopez-Martinez, C. and Grimalt, J. O.: Gulf Stream variability during marine](#)
1593 [isotope stage 3, Paleoceanography, 19, PA2011, doi:10.1029/2003PA000966, 2004.](#)

1594 [Vautravers, M. J., Bianchi, G. and Shackleton, N. J.: Subtropical NW Atlantic surface water variability during the](#)
1595 [last interglacial, in: Sirocko, F., Claussen, M., Sánchez-Goni, M. F., Litt, T. \(Eds.\), The Climate of Past](#)
1596 [Interglacials, Developm. in Quat. Sci., Elsevier, pp. 289–303, doi:10.1016/S1571-0866\(07\)80045-5,](#)
1597 [2007.](#)

1598 [Vellinga, M. and Wood, R. A.: Global Climatic Impacts of a Collapse of the Atlantic Thermohaline Circulation,](#)
1599 [Clim. Change, 54, 251–267, doi: 10.1023/A:1016168827653, 2002.](#)

1600 [Wang, C. and Lee, S.: Atlantic warm pool, Caribbean low-level jet, and their potential impact on Atlantic](#)
1601 [hurricanes, Geophys. Res. Lett., 34, doi:10.1029/2006GL028579, 2007.](#)

1602 [Wang, X., Auler, A. S., Edwards, R. L., Cheng, H., Cristalli, P. S., Smart, P. L., Richards, D. A., Shen, C.-C.:](#)
1603 [Wet periods in northeastern Brazil over the past 210 kyr linked to distant climate anomalies, Nature, 432,](#)
1604 [740, doi:10.1038/nature03067, 2004.](#)

Deleted: Slowey, N. C., Henderson, G. M. and Curry, W. B.: Direct U–Th dating of marine sediments from the two most recent interglacial periods, Nature, 383, 242, doi:10.1038/383242a0, 1996.

Deleted: Spratt, R. M. and Lisiecki, L. E.: A Late Pleistocene sea level stack, Clim. Past, 12, 1079–1092, doi:10.5194/cp-12-1079-2016, 2016.

Deleted: Tucker, M. E. and Bathurst, R. G.: Carbonate diagenesis, John Wiley and Sons, 2009.

Deleted:

1616 [Williams, S. C.: Stratigraphy, Facies Evolution and Diagenesis of Late Cenozoic Lime- stones and Dolomites,](#)
1617 [Little Bahama Bank, Bahamas, Univ. Miami, Coral Gables FL, 1985.](#)
1618 [Wilson, P. A. and Roberts, H. H.: Density cascading: off-shelf sediment transport, evidence and implications,](#)
1619 [Bahama Banks, J. Sedim. Res., 65\(1\), 45-56, 1995.](#)
1620 [Yarincik, K. M., Murray, R. W., Peterson, L. C.: Climatically sensitive eolian and hemipelagic deposition in the](#)
1621 [Cariaco Basin, Venezuela, over the past 578,000 years: Results from Al/Ti and K/Al, Paleoceanography,](#)
1622 [15, 210–228, doi:10.1029/1999PA900048, 2000.](#)
1623 [Zhang, R.: Anticorrelated multidecadal variations between surface and subsurface tropical North Atlantic,](#)
1624 [Geophys. Res. Lett., 34, doi:10.1029/2007GL030225, 2007.](#)
1625 [Zhuravleva, A., Bauch, H. A. and Spielhagen, R. F.: Atlantic water heat transfer through the Arctic Gateway](#)
1626 [\(Fram Strait\) during the Last Interglacial, Glob. Planet. Change, 157, 232–243,](#)
1627 [doi:10.1016/j.gloplacha.2017.09.005, 2017a.](#)
1628 Zhuravleva, A., Bauch, H.A. and Van Nieuwenhove, N.: Last Interglacial (MIS5e) hydrographic shifts linked to
1629 meltwater discharges from the East Greenland margin, Quat. Sci. Rev., 164, 95–109,
1630 doi:10.1016/j.quascirev.2017.03.026, [2017b.](#)
1631 [Ziegler, M., Nürnberg, D., Karas, C., Tiedemann, R. and Lourens, L. J.: Persistent summer expansion of the](#)
1632 [Atlantic Warm Pool during glacial abrupt cold events, Nature Geosci., 1, 601, doi:10.1038/ngeo277,](#)
1633 [2008.](#)
1634
1635

Deleted: ¶

Deleted: ¶

Deleted: 2017a

Deleted: Zhuravleva, A., Bauch, H. A. and Spielhagen, R. F.: Atlantic water heat transfer through the Arctic Gateway (Fram Strait) during the Last Interglacial, Glob. Planet. Change, 157, 232–243, doi:10.1016/j.gloplacha.2017.09.005, 2017b. ¶

Figure captions

Figure 1: Maps showing positions of investigated sediment records and oceanic/atmospheric circulation.

(a) Simplified surface water circulation in the (sub)tropical North Atlantic and positions of investigated core records: MD99-2202 (27°34.5' N, 78°57.9' W, 460 m water depth; *this study*), Ocean Drilling Program (ODP) Site 1002 (10°42.7' N, 65°10.2' W, 893 m water depth; Gibson and Peterson, 2014), MD03-2664 (57°26.3' N, 48°36.4' W, 3442 m water depth, Galaasen et al., 2014) and PS1243 (69°22.3' N, 06°33.2' W, 2710 m water depth, Bauch et al., 2012). (b) Relative abundances of the tropical foraminifera *G. sacculifer* and *G. ruber* (pink) (Siccha and Kučera, 2017) and positions of the Intertropical Convergence Zone (ITCZ) during boreal winter and summer. (c) Summer and winter hydrographic sections (as defined by the black line in b), showing temperature and salinity obtained from the World Ocean Atlas (Levitus et al., 2013). Vertical bars denote calcification depths of *G. ruber* (white) and *G. truncatulinoides* (dex). Note, that *G. truncatulinoides* (dex) reproduce in winter time and due to its life cycle with changing habitats (as shown with arrows) accumulate signals from different water depths. Maps are created using Ocean Data View (Schlitzer, 2016).

Figure 2: The age model for MIS 5 in core MD99-2202. The temporal framework is based on alignment of (b) planktic $\delta^{18}\text{O}$ values (Lantzsich et al., 2007) and (d) relative abundance record of *Globigerinoides* species with (a) global benthic isotope stack LS16 (Lisiecki and Stern, 2016). (c) Aragonite content in black (Lantzsich et al., 2007) and normalized elemental intensities of Sr in lilac as well as (e) relative abundances of *G. menardii* are shown to support the stratigraphic subdivision of MIS 5.

Figure 3: XRF-scan results, sedimentological and foraminiferal data from core MD99-2202 for the period 140-100 ka. (a) $\delta^{18}\text{O}$ values in *G. ruber* (white); (b) aragonite content; (a-b) is from Lantzsich et al. (2007). Normalized elemental intensities of (c) Sr, (e) Ca and (f) Cl, (d) Sr/Ca intensity ratio (truncated at 0.6) and (g) absolute abundances of *G. menardii* per sample. Green bars denote core intervals with biased elemental intensities due to high seawater content. The inferred platform flooding interval (see text) is consistent with the enhanced production of Sr-rich aragonite needles and a RSL above -6 m (d). T2 – refers to the position of the penultimate deglaciation (Termination 2).

Figure 4: Proxy records from core MD99-2202 over the last interglacial cycle. (a) $\delta^{18}\text{O}$ values in *G. ruber* (white) (Lantzsich et al., 2007), (b) $\delta^{18}\text{O}$ values in *G. truncatulinoides* (dex) (black) and *G. inflata* (blue), (c-d)

Deleted: core ...ediment records and oceanic/atmospheric/oceanic...circulation. (A ... [29]

Deleted: .

Deleted: sediment ...ore records: MD99-2202 (27°34.5' N, 78°57.9' ... , 460 m water depth; *this study*), Ocean Drilling Program (ODP) Site 1002 (10°42.7' ... , 65°10.2' W, 893 m water depth; Gibson and Peterson, 2014), MD03-2664 and...ODP Site 1063 (...57°26.3' N, 48°36.4' W, 3442 m water depth, Galaasen et al., 2014) and PS1243 (69°22.3' N, 06°33.2' W, 2710 m water depth, Bauch et al., 2012)... (B ... [30]

Deleted: i...ntertropical Cc...nvergence Zz ... [31]

Deleted: C...) Summer and winter hydrographic sections (as defined by the black line in B...), showing temperature and salinity obtained from the World Ocean Atlas (Levitus et al., 2013). Vertical bars denote calcification depths of *G. ruber* (white) and *G. truncatulinoides* (dex), respectively [32]

Deleted: . NEC – North Equatorial Current, AC – Antilles Current, FC – Florida Current, STG – subtropical gyre... Maps are created using Ocean Data View (Schlitzer, 2016) [33]

Deleted: Figure 2: XRF-scan results and sedimentological data from core MD99-2202. (A) $\delta^{18}\text{O}$ values in *G. ruber* (white); (B) aragonite content; (C) fraction with grain size <63 μm ; (A-C) is from Lantzsich et al. (2007). Normalized elemental intensities of (D) Sr, (E) Ca and (G) Cl and (F) Sr/Ca intensity ratio. Green bars denote core intervals with biased elemental intensities due to inferred high seawater content (see main text). The white arrows mark a coherent change in sedimentological proxies at 350 cm (B-D).

Deleted: **Figure 3...: The age model for MIS 5 Chronology...of...n core MD99-2202...** The temporal framework Age model...is based on alignment of (b) planktic $\delta^{18}\text{O}$ values (Lantzsich et al., 2007) and (D) ...d) relative abundance record of *Globigerinoides* species and (B) planktic $\delta^{18}\text{O}$ values (Lantzsich et al., 2007) ...ith (A...) global benthic isotope stack LS16 (Lisiecki and Stern, 2016). (C...) Aragonite content in black (Lantzsich et al., 2007) and normalized elemental intensities of Sr in lilac and ...s well as (E...) relative abundances of *G. menardii* and *G. menardii flexuosa* ... [34]

Deleted: 2...: XRF-scan results, and...sedimentological and foraminiferal data from core MD99-2202 for the period 140-100 ka. (a) $\delta^{18}\text{O}$ values in *G. ruber* (white); (b) aragonite content; (C) fraction with grain size <63 μm ; ...a-C...) is from Lantzsich et al. (2007). Normalized elemental intensities of (D...) Sr, (e) Ca and (G...) Cl, and...(F...) Sr/Ca intensity ratio (truncated at 0.6) and (g) absolute abundances of *G. menardii* per sample. Green bars denote core intervals with biased elemental intensities due to high [35]

Deleted: Figure 2: XRF-scan results and sedimentological data from core MD99-2202. (A) $\delta^{18}\text{O}$ values in *G. ruber* (white); (B) aragonite content; (C) fraction with grain size <63 μm ; (A-C) is from Lantzsich et al. (2007). Normalized elemental intensities of (D) Sr, (E) Ca and (G) Cl and (F) Sr/Ca intensity ratio. Green bars denote core intervals with biased elemental intensities due to high [36]

Deleted: 5...: Proxy records from core MD99-2202 over the last interglacial cycle. (A...) $\delta^{18}\text{O}$ values in *G. ruber* (white) (Lantzsich et al., 2007), (B...) $\delta^{18}\text{O}$ values in *G. truncatulinoides* (dex) (black) and *G. inflata* (blue), (C...) [37]

isotopic gradients between $\delta^{18}\text{O}$ values in *G. ruber* (white) and *G. truncatulinoides* (dex) and *G. ruber* (white) and *G. inflata*, respectively. (e-f) relative abundances of *G. inflata* and *G. truncatulinoides* (dex), respectively, (g) normalized Fe intensities. Also shown in (e) and (f) are modern relative foraminiferal abundances (average value $\pm 1\sigma$) around Bahama Bank, computed using 7 nearest samples from Siccha and Kučera (2017) database. T2 – Termination 2.

Deleted: $\Delta\delta^{18}\text{O}$...etween $\delta^{18}\text{O}$ values in *G. ruber* (white) and *G. truncatulinoides* (dex) and *G. ruber* (white) and *G. inflata*, ... respectively, (D...-f) relative abundances of *G. inflata* and normalized Fe intensities, (E) relative abundances of *truncatulinoides* (dex) (green) and *G. truncatulinoides* (sin) (black)... respectively, ... (g) normalized Fe intensities (F) relative abundances of *G. falconensis* (violet) and *G. inflata* (black)... Also shown in (E...) and (F...) are modern relative foraminiferal abundances... (average value $\pm 1\sigma$) around Bahama Bank, computed using 7 nearest samples from Siccha and Kučera (2017) database. Shaded in lilac is the platform flooding interval (as defined in Fig. 4) [38]

Figure 5: Relative abundances of main *Globigerinoides* species in core MD99-2202 over the last interglacial cycle. (a) $\delta^{18}\text{O}$ values in *G. ruber* (white) (Lantzsch et al., 2007), relative abundances of (b) *G. sacculifer*, (c) *G. ruber* (pink), (d) *G. conglobatus* and (e) *G. ruber* (white). Also shown in (b-e) are modern relative foraminiferal abundances (average value $\pm 1\sigma$) around Bahama Bank, computed using 7 nearest samples from Siccha and Kučera (2017) database. T2 – Termination 2.

Deleted: 6.... Relative abundances...of main *Globigerinoides* species in core MD99-2202 over the last interglacial cycle. (A...) $\delta^{18}\text{O}$ values in *G. ruber* (white) (Lantzsch et al., 2007), relative abundances...of (B...) *G. sacculifer*, (C...) *G. ruber* (pink), (D...) *G. conglobatus* and... (E...) *G. ruber* (white). Also shown in (B...-E...) are modern relative foraminiferal abundances... (average value $\pm 1\sigma$) around Bahama Bank, computed using 7 nearest samples from Siccha and Kučera (2017) database. Shaded in lilac is the platform flooding interval (as defined in Fig. 4) [39]

Figure 6: Comparison of proxy records from tropical, subtropical and subpolar North Atlantic over the last interglacial cycle. (b) $\delta^{18}\text{O}$ values in *G. ruber* (white) in core MD99-2202 (Lantzsch et al., 2007), (c) relative abundances of the tropical species *G. sacculifer* and *G. ruber* (pink) in core MD99-2202, (d) molybdenum record from ODP Site 1002 (Gibson and Peterson, 2014), (e) $\delta^{13}\text{C}$ values measured in benthic foraminifera from core MD03-2664 (Galaasen et al., 2014, age model is from Zhuravleva et al., 2017b), (f) Ice-rafted debris in core PS1243 (Bauch et al., 2012, age model is from Zhuravleva et al., 2017b). Also shown is (a) boreal summer insolation (21 June, 30° N), computed with AnalySeries 2.0.8 (Paillard et al., 1996) using Laskar et al. (2004) data. Shown in (c) are modern relative abundances of *G. sacculifer* and *G. ruber* (pink) (average value $\pm 1\sigma$) around Bahama Bank, computed using 7 nearest samples from Siccha and Kučera (2017) database. The blue band suggests correlation of events (Younger Dryas-like cooling), across tropical, subtropical and subpolar North Atlantic (see text). T2 – Termination 2.

Deleted: 7.... Comparison of proxy records from (sub)...ropical, subtropical and subpolar North...Atlantic over the last interglacial cycle. (A) ...b) $\delta^{18}\text{O}$ values in *G. ruber* (white) in core MD99-2202 (Lantzsch et al., 2007), (B...) relative abundances of the tropical species *G. sacculifer* and *G. ruber* (pink) in core MD99-2202, (C) boreal summer insolation (21 June, 30° N), computed with AnalySeries 2.0.8 (Paillard et al., 1996) using Laskar et al. (2004) data, ...D...) molybdenum (Mo) ...ecord from ODP Site 1002 (Gibson and Peterson, 2014), (E...-F... $\delta^{13}\text{C}$ values measured in benthic foraminifera from core MD03-2664 (Galaasen et al., 2014, age model is from Zhuravleva et al., 2017b), (f) Ice-rafted debris in core PS1243 (Bauch et al., 2012, age model is from Zhuravleva et al., 2017b) and relative abundances of *G. ruber* (total) and *G. sacculifer* from ODP Site 1063 (Deaney et al., 2017)... Also shown is (a) boreal summer insolation (21 June, 30° N), computed with AnalySeries 2.0.8 (Paillard et al., 1996) using Laskar et al. (2004) data. Also s...hown in (B...) are modern relative abundances of *G. sacculifer* and *G. ruber* (pink) (average value $\pm 1\sigma$) around Bahama Bank, computed using 7 nearest samples from Siccha and Kučera (2017) database. The blue arrows ...and the dashed line ...uggests correlation of events ((so-called ...ounger Dryas- type ...ike cooling))...in...cross the ...ropical, subtropical and tropical...ubpolar North...Atlantic (see text). Shaded in lilac is the platform flooding interval (as defined in Fig. 4). ... [40]